



Group 3 Metal Complexes Supported by Tridentate Pyridine- and Thiophene-Linked Bis(naphtholate) Ligands: Synthesis, Structure, and Use in Stereo-selective Ring-Opening Polymerization of Racemic Lactide and beta-Butyrolactone

Ekaterina Grunova, Evgueni Kirillov, Thierry Roisnel, Jean-François Carpentier

► To cite this version:

Ekaterina Grunova, Evgueni Kirillov, Thierry Roisnel, Jean-François Carpentier. Group 3 Metal Complexes Supported by Tridentate Pyridine- and Thiophene-Linked Bis(naphtholate) Ligands: Synthesis, Structure, and Use in Stereo-selective Ring-Opening Polymerization of Racemic Lactide and beta-Butyrolactone. Dalton Transactions, 2010, 39 (29), pp.6739-6752. 10.1039/b920283h . hal-00492625

HAL Id: hal-00492625

<https://hal.science/hal-00492625>

Submitted on 16 Jan 2014

HAL is a multi-disciplinary open access archive for the deposit and dissemination of scientific research documents, whether they are published or not. The documents may come from teaching and research institutions in France or abroad, or from public or private research centers.

L'archive ouverte pluridisciplinaire **HAL**, est destinée au dépôt et à la diffusion de documents scientifiques de niveau recherche, publiés ou non, émanant des établissements d'enseignement et de recherche français ou étrangers, des laboratoires publics ou privés.

Group 3 metal complexes supported by tridentate pyridine- and thiophene-linked bis(naphtholate) ligands: synthesis, structure, and use in stereoselective ring-opening polymerization of racemic lactide and β -butyrolactone†

Ekaterina Grunova, Evgueni Kirillov,* Thierry Roisnel and Jean-François Carpentier*

Received 29th September 2009, Accepted 25th November 2009

First published as an Advance Article on the web 7th January 2010

DOI: 10.1039/b920283h

Scandium, yttrium and lanthanum amido complexes supported by tridentate bis(*ortho*-silyl-substituted naphtholate)-donor ligands ($\{\text{ONO}^{\text{SiPh}_3}\}^{2-}$ and $\{\text{ONO}^{\text{Si}^i\text{BuMe}_2}\}^{2-}$, donor = 2,6-pyridine; $\{\text{OSO}^{\text{SiPh}_3}\}^{2-}$, donor = 2,5-thiophene) have been prepared in high yields (72–96%) by reaction of the corresponding pro-ligand $\{\text{OZO}^{\text{SiR}_3}\}\text{H}_2$ and $\text{Ln}[\text{N}(\text{SiHMe}_2)_2](\text{THF})_n$ precursor. The solid-state structures of $\{\text{ONO}^{\text{SiPh}_3}\}\text{La}[\text{N}(\text{SiHMe}_2)_2](\text{THF})$ (**3**), $\{\text{ONO}^{\text{Si}^i\text{BuMe}_2}\}\text{Ln}[\text{N}(\text{SiHMe}_2)_2](\text{THF})$ ($\text{Ln} = \text{Sc}$, **4**; Y , **5**) and $\{\text{OSO}^{\text{SiPh}_3}\}\text{Ln}[\text{N}(\text{SiHMe}_2)_2](\text{THF})$ ($\text{Ln} = \text{Sc}$, **7**; La , **9**) have been determined by single-crystal X-ray diffraction studies. In all five complexes, the naphtholate rings twist in the same direction from the plane of the pyridine or thiophene linker, to give rise to C_s -symmetric (non crystallographic) structures. Compounds **1–9** are single-site initiators for the ring-opening polymerization (ROP) of *racemic* lactide (*rac*-LA) at 20 °C, affording poly(lactides) (PLAs) with relatively narrow polydispersities and molecular weights in good agreement with calculated values. When carried out in THF, the polymerizations afforded heterotactic-enriched PLAs (P_r up to 0.93), while atactic polymers are formed in toluene. Compounds **1–3** and **7–9**, having *o*-SiPh₃ substituents on the naphtholate rings, are also active for the ROP of *racemic* β -butyrolactone at 20–50 °C, to form syndiotactic-enriched poly(3-hydroxybutyrate)s (PHBs) (P_r up to 0.87) when using toluene as the solvent, whereas atactic polymers were obtained in THF. The nature of the metal center (Sc, Y, La), the central linker in the ligand framework (pyridine, thiophene), and the *ortho*-silyl substituent (SiPh₃, SiMe₂*t*Bu) significantly affect the degree of stereocontrol in those polymerizations.

Introduction

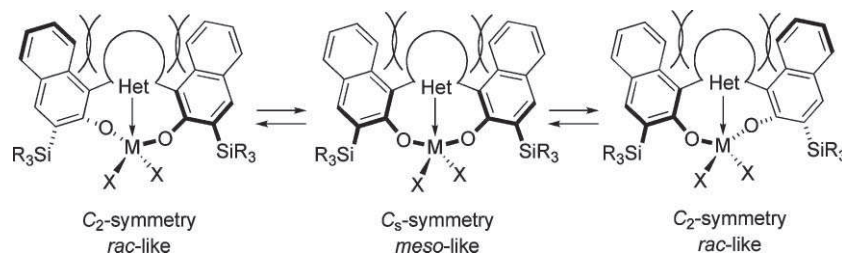
Phenolates (aryloxides) combined with other donor atoms (N, S, O...) are common multidentate ligands for early transition metals,¹ which have met with much success in the development of post(non)-metallocenes for polymerization catalysis. Discrete group 3–6 metal complexes bearing various bidentate,² tridentate,³ and tetradentate⁴ phenolate-based ligands have demonstrated high performances (*i.e.*, catalytic activity, degree of control, stereoselectivity) in the oligomerization/polymerization of ethylene and α -olefins.⁵ More recently, this class of ligands, particularly the bis(phenolate)s, has been investigated in the ring-opening polymerization (ROP) of cyclic esters, such as lactide, for the preparation of biocompatible polymers,⁶ mostly in combination

with group 3 (lanthanides)⁷ and also to a lesser extent group 4 metals.⁸

Of particular interest are tridentate ligands $\{\text{OZO}\}^{2-}$ where a rigid flat central donor of the “L”-type is flanked by two phenolate rings, because such “LX₂”-type ligands can confer various symmetries at the metal center. For instance, bis(phenolate) ligands having a 2,6-pyridine, 2,5-furan or 2,5-thiophene linker have been shown to bind to iron(III), copper(II), aluminium(III),⁹ and Ti(IV)^{3f} in a C_2 (*rac*) fashion, while they bind to zirconium(IV)^{3d,e,f} and boron(III)¹⁰ in a C_s (*meso*) or C_1 fashion. Static or dynamic control over these diverse symmetries is of great interest in polymerization catalysis, as it may eventually give rise to polymers with stereoregular microstructures.^{5,6} On this principle, we have recently prepared sterically demanding silyl *ortho*-substituted tridentate 2,6-bis(naphtholate)pyridine ($\{\text{ONO}^{\text{SiR}_3}\}^{2-}$, SiR₃ = SiPh₃, SiMe₂*t*Bu) and 2,5-bis(naphtholate)thiophene ($\{\text{OSO}^{\text{SiPh}_3}\}^{2-}$) ligands and studied their corresponding group 4 metal (Ti, Zr, Hf) complexes.¹¹ An anticipated key feature of these ligands was the possibility for firm stereoselective coordination to the metal center provided by the non-coplanar orientation of the bridging heterocyclic and adjacent naphthoxy groups, due to steric repulsion between protons at *meta* and 8-positions¹² of these moieties, respectively. In fact, X-ray diffraction studies revealed that, in the solid state, the latter group 4 metal complexes adopt either *rac*-like or *meso*-like binding of the ligand, while VT NMR spectroscopy studies in toluene

Catalysis and Organometallics, UMR 6226 Sciences Chimiques de Rennes, CNRS-University of Rennes 1, 35042, Rennes, Cedex, (France). E-mail: jean-francois.carpentier@univ-rennes1.fr, evgueni.kirillov@univ-rennes1.fr; Fax: (+33)(0)223-236-939

† Electronic supplementary information (ESI) available: cif files for crystal structure determinations of complexes **3–5**, **7**, **9** and **10**, ORTEP views and main bond distances and angles for complexes **3**, **5** and **9**, and representative ¹H NMR and ¹³C NMR spectra of PLA and PHB. CCDC reference numbers 752787, 752788, 752789, 752790, 752791 and 752792. For ESI and crystallographic data in CIF or other electronic format see DOI: 10.1039/b920283h



Scheme 1 Examples of common geometries in $\{\text{OZO}^{\text{SiR}_3}\}\text{M}$ complexes and corresponding dynamic processes.

solution indicated that such complexes exist as *rac* and *meso* stereoisomers that interconvert relatively easily (activation parameters: $\Delta H^\ddagger = 12.9(7)$ – $13.4(8)$ kcal mol $^{-1}$ and $\Delta S^\ddagger = -3(1)$ to $-7(1)$ cal mol $^{-1}$ K $^{-1}$) (Scheme 1). Yet, these systems showed disappointing catalytic performance in propylene polymerization (upon activation with MAO), leading at best to atactic oligomers with poor activity.

This naphthoxy-based $\{\text{OZO}^{\text{SiR}_3}\}^{2-}$ ligand platform is also of potential interest to group 3 metal chemistry and related ROP catalysis of chiral (racemic) cyclic esters, for several reasons: First, such chelating ligands should accommodate metal centers with quite different ionic radii; this should allow studying in more detail the impact of the latter parameter, as well as the influence of hard ($Z = \text{N}$) vs. soft ($Z = \text{S}$) donating heteroatom and *ortho*-silyl groups over the polymerization course (activity, control). Such data are still necessary because no clear rationale exists yet to account for the reported behavior of group 3 metal catalysts in ROP of cyclic esters.⁶ Second, yet much more challenging, if complexes with different symmetries (e.g., with a C_2 -, C_s -symmetric ligand) are attainable and if a *reasonably easy* dynamic interconversion between such *geometrically stable* isomers, e.g. *rac* and *meso* occurs, original multiblock microstructures (varying by the nature or degree of tacticity) could be accessed *via* “oscillating” polymerization.

Accordingly, we describe herein the coordination chemistry of $\{\text{OZO}^{\text{SiR}_3}\}^{2-}$ ligands with group 3 metals ($\text{Ln} = \text{Sc}, \text{Y}, \text{La}$). The performance of the amido compounds $\{\text{OZO}^{\text{SiR}_3}\}\text{Ln}[\text{N}(\text{SiHMe}_2)_2](\text{THF})$ in the stereoselective ROP of racemic lactide and racemic- β -butyrolactone¹³ is also reported.

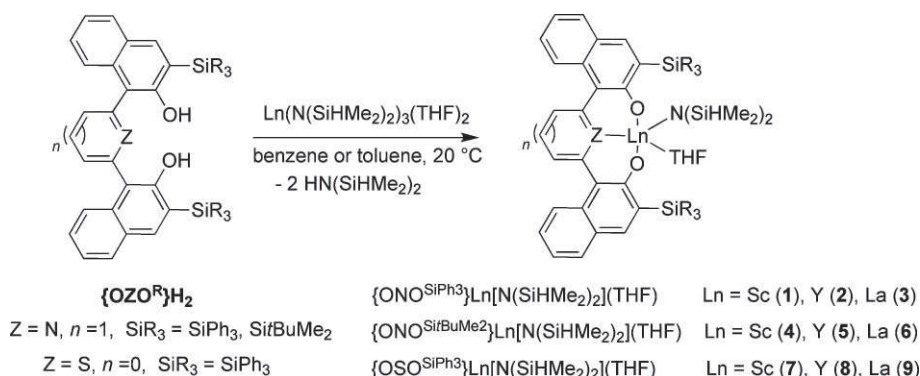
Results and discussion

Preparation of scandium, yttrium and lanthanum complexes supported by tridentate bis(naphtholate)-donor ligands

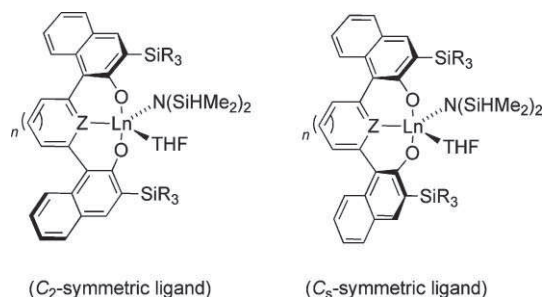
Scandium, yttrium and lanthanum complexes were prepared by amine elimination in reaction of the corresponding tris(dimethylsilyl)amido metal group 3 precursors and bis(naphthol)-donor pro-ligands $\{\text{OZO}^{\text{SiR}_3}\}\text{H}_2$ ¹¹ (Scheme 2). The reactions proceeded cleanly at room temperature in benzene or toluene solutions, as evidenced by NMR monitoring. Complexes **1–5** and **7–9** were isolated in 72–96% yields as pale yellow microcrystalline powders, which are air-sensitive and readily soluble in most usual organic solvents. Complex **6** was generated *in situ* for further use in catalysis (*vide infra*), but not isolated.

A coordinated THF molecule was systematically observed by ^1H and ^{13}C NMR spectroscopy for all complexes. This observation, in line with the mononuclear structures in the solid state for such amido group 3 metal compounds (*vide infra*) and the unlikely bridging modes of the bulky $\text{N}(\text{SiHMe}_2)_2^-$ and $\{\text{OZO}^{\text{SiR}_3}\}^{2-}$ ligands, suggests that $\{\text{OZO}^{\text{SiR}_3}\}\text{Ln}[\text{N}(\text{SiHMe}_2)_2](\text{THF})$ compounds are mononuclear and five-coordinate in benzene or toluene solution. The chemical shifts for the SiH (δ 4.29–4.76 ppm at 298 K in benzene- d_6), which are shifted upfield compared to the chemical shift in the corresponding $[\text{Ln}\{\text{N}(\text{SiHMe}_2)_2\}_3(\text{THF})_2]$ precursors (δ 4.94–5.02 ppm), argue against a significant $\beta(\text{Si}-\text{H})$ agostic interaction with the metal center in solution (*vide infra*).¹⁴

As mentioned in the Introduction section, these bis(naphtholate)-donor ligands can achieve, in principle, a variety of binding geometries, two of them being most common (C_2 , C_s ; Scheme 3),^{3f,11,15} that should be distinguishable by NMR



Scheme 2



Scheme 3 Geometries observed in $\{\text{OZO}^{\text{SiR}_3}\}\text{Ln}[\text{N}(\text{SiHMe}_2)_2](\text{THF})$ complexes.

spectroscopy. Such analysis is, however, hampered in the present case by the complicated pattern of resonances associated with the naphtholate rings in the ^1H NMR spectra, especially when SiPh_3 substituents are present. More informative data were obtained from variable-temperature NMR experiments on the complexes bearing $\text{Si}i\text{BuMe}_2$ substituents at the naphtholate rings. In fact, the ^1H NMR data for both **4** and **5** are consistent with the

existence, on the NMR time scale, of a single species with a C_s-symmetrically bound ligand¹⁵ in toluene in the temperature range 223–338 K (Fig. 1 and 2). No additional resonances, in particular in the aromatic region, were observed that could account for the presence [within experimental accuracy] of a second stereoisomer. Relevant features of these VT NMR spectra include, for both compounds, one sharp singlet resonance [b] for the methyl hydrogens of the $\text{Si}i\text{BuMe}_2$ groups in the high temperature spectra which decoalesced to give two sharp singlet resonances in the low temperature spectra. At the same time, as best seen in yttrium compound **5**: the α -THF methylene hydrogens appear as a [broadened] singlet [e] in the high temperature spectrum and decoalesced in two well-resolved resonances [e/e'] at 233 K.¹⁶ We tentatively interpret those dynamic phenomena, which are reversible upon increasing or decreasing the temperature, in relation with rotation of the coordinated THF molecule (and fluxionality within the latter cycle). Site exchange (of THF and the amide ligands, which would imply THF dissociation) seems unlikely as this would generate species in different environments that should be distinguished by ^1H NMR at low temperature, which is not the case (*vide supra*).

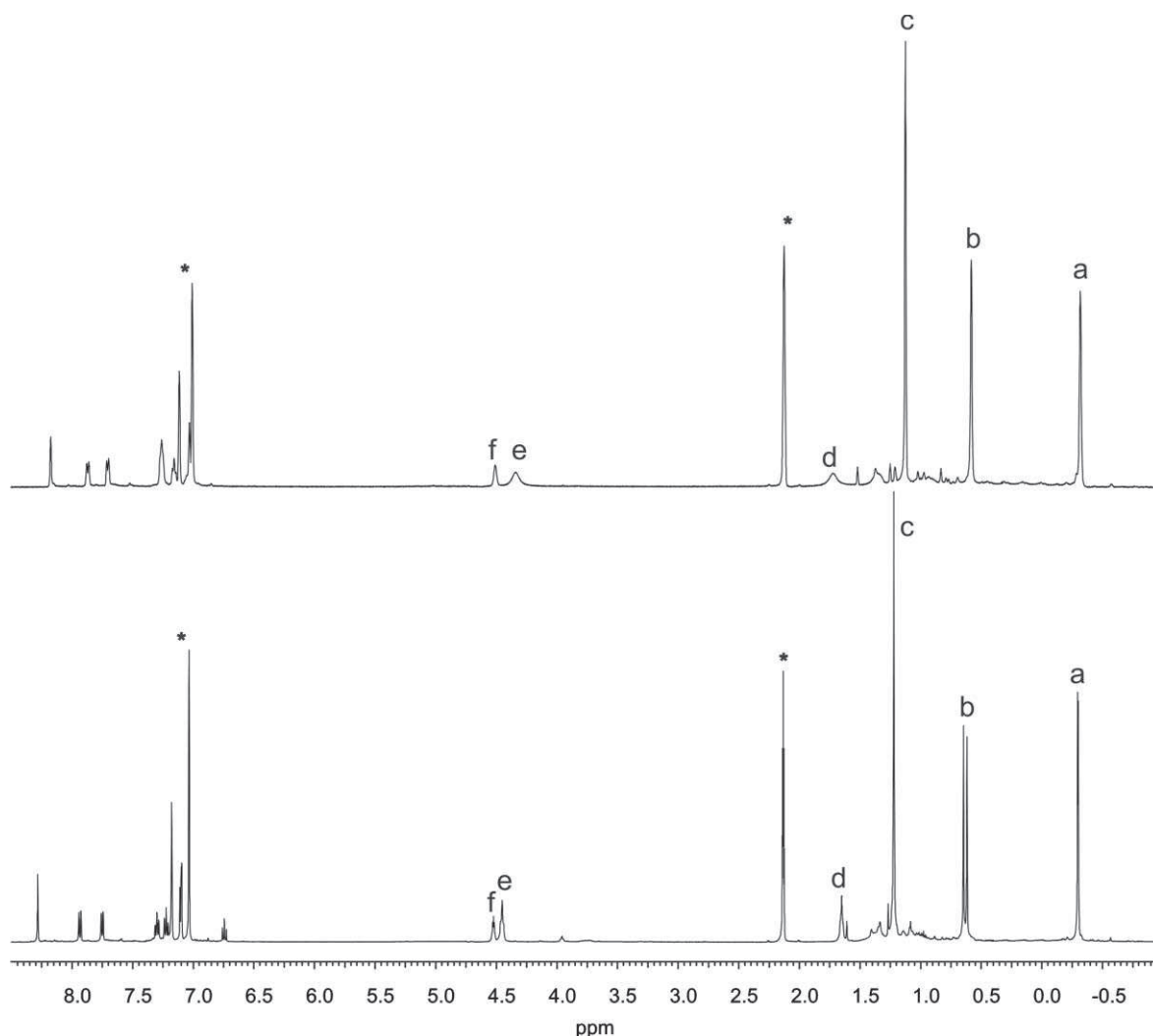


Fig. 1 VT- ^1H NMR spectra (500 MHz, toluene- d_8) of $\{\text{ONO}^{\text{Si}i\text{BuMe}_2}\}\text{Sc}[\text{N}(\text{SiHMe}_2)_2](\text{THF})$ (**4**); bottom, 223 K; top, 338 K. (a) SiHMe_2 ; (b) $\text{Si}i\text{BuMe}_2$; (c) $\text{Si}i\text{BuMe}_2$; (d) β -THF; (e) α -THF; (f) SiHMe_2 (* refers to residual solvent resonances).

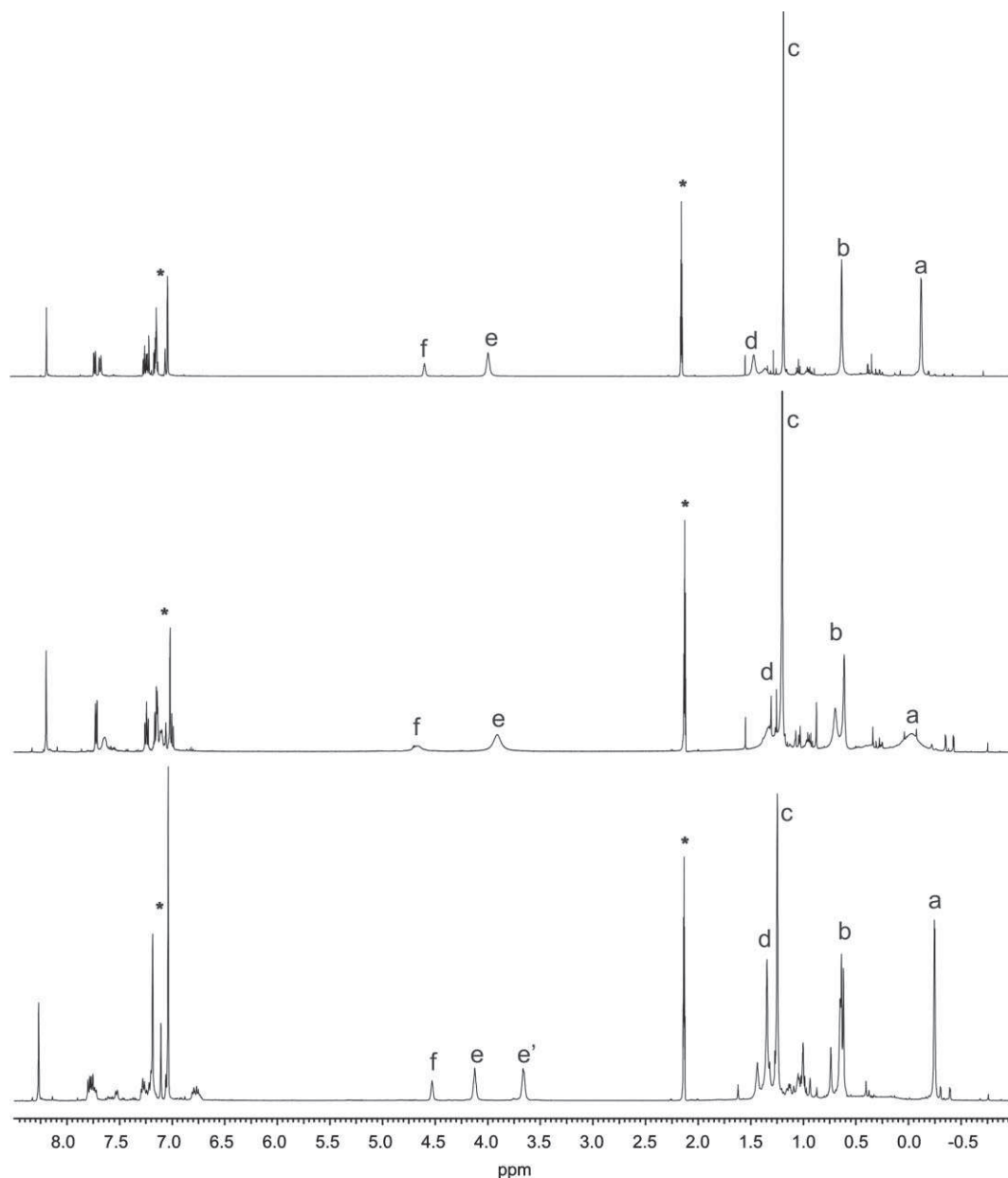


Fig. 2 VT- ^1H NMR spectra (500 MHz, toluene- d_8) of $\{\text{ONO}^{\text{SiHMe}_2}\}\text{Y}[\text{N}(\text{SiHMe}_2)_2](\text{THF})$ (**5**); bottom, 233 K; middle, 296 K; top, 338 K. (a) SiHMe_2 ; (b) Si^iBuMe_2 ; (c) Si^tBuMe_2 ; (d) β -THF; (e) α -THF; (f) SiHMe_2 (* refers to residual solvent resonances).

Solid state structures of scandium, yttrium and lanthanum complexes supported by tridentate bis(naphtholate)-donor ligands

Determination of the binding modes of the bis(naphtholate)-donor ligands in these complexes is more straightforward from single-crystal X-ray diffraction studies, although these observations in the solid state may not necessarily reflect the actual geometries in solution. Crystals suitable for X-ray diffraction studies were successfully grown from concentrated benzene solution at room temperature for compounds **3–5**, **7**, and **9**. The main crystallographic details are reported in Table 1. The molecular structures of **4** and **7**, and selected bond distances and angles for these compounds are given in Fig. 3 and 4, respectively. Structures and geometric factors for the other compounds are quite similar and available as ESI.†

All five complexes show a distorted trigonal-bipyramidal geometry at the metal center, which is five-coordinated by the $\{\text{OZO}^{\text{SiR}_3}\}^{2-}$ ligand, the THF molecule and the dimethylsilylamido group. Yet, β -agostic interactions between one of the Si–H of the latter amido group and the metal center are evidenced in all complexes by close $\text{M}\cdots\text{H}(\text{Si})$ contacts (2.818–3.129 Å) and $\text{M}\cdots\text{Si}(\text{H})$ contacts (3.134–3.370 Å) (Table 2). These agostic interactions are confirmed by the observation of a more obtuse M–Si–N bond angle (102.4(5)–116.4(2)°). These interactions remain, however, overall weak; this is attested by the Si–N–Si bond angles of 122.1(2)–130.6(2)° that are slightly larger than the angle of 120° for ideal sp^2 hybridization and that fall into the upper range of values reported for Si–N–Si angles (119.93–129.58°).¹⁷

Table 1 Summary of crystal and refinement data for compounds **3–5**, **7**, **9** and **10** (all data were collected at 100 K)

	3	4·2.5(C₆H₆)	5·2.5(C₆H₆)	7·4(C₆H₆)	9·0.5(C₆H₁₄)	10·4(C₆H₆)
Empirical formula	C ₆₉ H ₆₅ LaN ₂ O ₃ Si ₄	C ₄₅ H ₆₅ N ₂ O ₃ ScSi ₄ ·2.5(C ₆ H ₆)	C ₄₅ H ₆₅ YN ₂ O ₃ Si ₄ ·2.5(C ₆ H ₆)	C ₆₈ H ₆₄ NO ₃ SScSi ₄ ·4(C ₆ H ₆)	C ₆₈ H ₆₄ LaNO ₃ SSi ₄ ·0.5(C ₆ H ₁₄)	C ₁₂₆ H ₁₀₀ La ₂ N ₂ O ₉ Si ₄ ·4(C ₆ H ₆)
Formula weight	1221.5	1034.58	1078.53	1445.01	1269.62	2488.69
Crystal system	Triclinic	Monoclinic	Monoclinic	Triclinic	Monoclinic	Orthorhombic
Space group	<i>P</i> -1	<i>P</i> 2 ₁ / <i>n</i>	<i>P</i> 2 ₁ / <i>n</i>	<i>P</i> -1	<i>C</i> 2/ <i>c</i>	<i>P</i> cab
<i>a</i> /Å	11.5427(13)	11.2092(6)	11.2947(9)	12.3960(7)	38.9355(14)	22.4713(9)
<i>b</i> /Å	13.2146(15)	23.4248(12)	23.4235(17)	15.9382(10)	15.5687(6)	29.6425(13)
<i>c</i> /Å	21.910(3)	22.6197(11)	22.7434(17)	21.8083(14)	22.9647(8)	39.1800(14)
α (°)	72.404(6)	90	90	103.867(4)	90	90
β (°)	88.235(6)	94.018(3)	93.324(4)	98.581(4)	113.803(2)	90
γ (°)	76.123(7)	90	90	106.022(3)	90	90
Volume/Å ³	3089.5(7)	5924.7(5)	6006.9(8)	3912.1(4)	12736.5(8)	26098.0(18)
<i>Z</i>	2	4	4	2	8	8
Density, Mg m ⁻³	1.313	1.160	1.193	1.227	1.324	1.264
μ /mm ⁻¹	0.816	0.248	1.093	0.233	0.826	0.741
<i>F</i> (000)	1260	2220	2292	1528	5256	10192
Crystal size/mm	0.20 × 0.05 × 0.04	0.52 × 0.30 × 0.25	0.42 × 0.38 × 0.21	0.16 × 0.10 × 0.06	0.28 × 0.17 × 0.14	0.20 × 0.20 × 0.065
θ range, deg	2.53 to 21.42	3.48 to 27.48	3.44 to 27.47	3.42 to 27.48	3.41 to 27.48	3.41 to 27.45
Limiting indices	−14 ≤ <i>h</i> ≤ 14, −17 ≤ <i>k</i> ≤ 15, −28 ≤ <i>l</i> ≤ 28	−14 ≤ <i>h</i> ≤ 13, −30 ≤ <i>k</i> ≤ 30, −29 ≤ <i>l</i> ≤ 29	−14 ≤ <i>h</i> ≤ 14, −23 ≤ <i>k</i> ≤ 30, −29 ≤ <i>l</i> ≤ 29	−16 ≤ <i>h</i> ≤ 15, −20 ≤ <i>k</i> ≤ 20, −28 ≤ <i>l</i> ≤ 27	−50 ≤ <i>h</i> ≤ 35, −20 ≤ <i>k</i> ≤ 20, −29 ≤ <i>l</i> ≤ 29	−29 ≤ <i>h</i> ≤ 24, −37 ≤ <i>k</i> ≤ 38, −27 ≤ <i>l</i> ≤ 50
Reflec. collected	14021	63479	52124	43820	67600	151425
<i>R</i> _{int}	0.1200	0.0538	0.0534	0.1075	0.0618	0.1008
Reflec. unique	9954	13476	13601	17816	14447	29729
[<i>I</i> > 2σ(<i>I</i>)]						
Data/restraints/param.	14021/0/702	13476/0/651	13601/0/691	17816/0/917	14447/2/699	29729/477/1024
Goodness-of-fit on <i>F</i> ²	1.201	1.122	1.03	1.058	1.020	1.032
<i>R</i> ₁ [<i>I</i> > 2σ(<i>I</i>)]	0.1307(0.1753)	0.0635 (0.0754)	0.0413 (0.0713)	0.1013 (0.1762)	0.0426 (0.0693)	0.0828 (0.1255)
(all data)						
w <i>R</i> ₂ [<i>I</i> > 2σ(<i>I</i>)]	0.2464 (0.2678)	0.1121 (0.1174)	0.0848 (0.0943)	0.1621 (0.1917)	0.0900 (0.1018)	0.1829 (0.2032)
(all data)						
Largest diff. e Å ⁻³	2.444 and −4.305	0.528 and −0.688	0.735 and −0.591	0.545 and −0.577	1.605 and −0.996	1.984 and −1.388

Table 2 Close contacts (Å) and angles (deg) attesting of Si–H...M agostic interactions in compounds **3–5**, **7** and **9**

Compound	M...H(Si)	M...Si	M–Si–N	Si–N–Si
3	2.818 4.240	3.210 3.737	102.4(5) 119.2(7)	119.3(7)
4	3.095 3.912	3.213 3.264	116.4(1) 119.9(1)	123.5(1)
5	2.966 4.040	3.247 3.443	111.4(1) 116.7(2)	130.1(2)
7	3.023 3.428	3.134 3.336	112.6(2) 125.3(2)	122.1(2)
9	3.129 3.278	3.370 3.474	111.8(1) 117.6(2)	130.6(2)

In all five complexes, the naphtholate rings twist in the same direction from the plane of the linker to give rise to *C_s*-symmetric (non crystallographic) structures. The degree of twisting, as measured by the dihedral angle between the M–O bonds and the plane of the linker, ranges from 49 to 84°. In some complexes, this degree of twisting may differ considerably within the two naphtholate rings. This difference in the twist angles is especially marked for the lanthanum complexes (**3**, 49.2 and 63.3°; **9**, 73.3 and 84.0°). This might just reflect the more pronounced influence of crystal packing around a large and therefore less sterically hindered metal center.¹⁸ For a given ligand, *i.e.*, {ONO^{SiPh₃}}²⁻, the twist angles slightly increase from scandium (**4**, 52.4 and 55.0°) to

yttrium (**5**, 56.5 and 60.4°). As indicated by the minimal difference between the twist angles, the structural features of the naphtholate rings in scandium complexes {ONO^{SirBuMe₂}}Sc[N(SiHMe₂)₂](THF) (**4**, 52.4 and 55.0°) and {OSO^{SiPh₃}}Sc[N(SiHMe₂)₂](THF) (**7**, 51.9 and 53.3°) are very similar. Yet, as illustrated in Fig. 3 and 4, the pyridine and thiophene linkers coordinate quite differently in those complexes: the thiophene ring is almost perpendicular to the M–S vector (dihedral angle: **7**, 88.3°; **9**, 73.9°), while the pyridine ring is only slightly deviated from the M–N vector (dihedral angle: **3**, 156.6°; **4**, 152.8°; **5**, 152.5°). Similar features were observed for group 4 metal complexes of bis(phenolate)-donor ligands.^{3f}

The selective (at least in the solid state) *C_s* binding mode of these bis(naphtholate)-donor ligands with group 3 metals is in line with the *C_s* binding mode of analogous CMe₃ and CEt₃ *ortho*-substituted bis(phenolate)-donor ligands (donor = pyridine, thiophene, furan) observed by Bercaw *et al.* in a series of tantalum(v) complexes.¹⁹ On the other hand, it is in contrast with the *C₂* or *C₁* binding mode¹⁵ of the latter bis(phenolate)-donor ligands^{3f} and present bis(naphtholate)-donor ligands¹¹ in five-coordinate dibenzyl titanium(iv), zirconium(IV) and hafnium(IV) complexes. Only for six-coordinate group 4 metal complexes, which adopt a distorted octahedral geometry, those bis(phenolate)-donor and bis(naphtholate)-donor ligands gave rise to a *C_s* binding mode.^{3d,e,f,11} These observations indicate that the binding mode of this type of LX₂ ligand is not simply controlled either by the

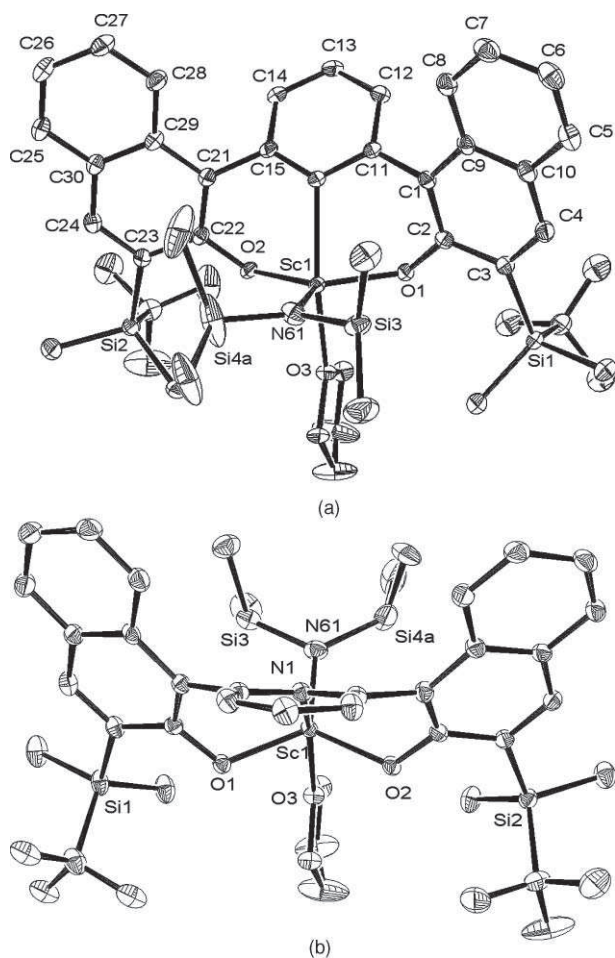


Fig. 3 ORTEP drawings of the structure of $\{\text{ONO}^{\text{Si}^i\text{BuMe}_2}\}\text{Sc}-[\text{N}(\text{SiHMe}_2)_2](\text{THF})$ (**4**) (50% ellipsoid probability; H atoms are omitted for clarity). Selected bond lengths (Å) and angles (deg.): Sc(1)–O(1), 2.0218(15); Sc(1)–O(2), 2.0067(15); Sc(1)–O(3), 2.1852(16); Sc(1)–N(1), 2.3094(18); Sc(1)–N(61), 2.052(2); O(2)–Sc(1)–O(1), 125.51(6); O(2)–Sc(1)–N(61), 116.21(7); O(1)–Sc(1)–N(61), 118.23(7); O(2)–Sc(1)–O(3), 87.13(6); O(1)–Sc(1)–O(3), 86.44(6); N(61)–Sc(1)–O(3), 99.33(7); O(2)–Sc(1)–N(1), 82.22(6); O(1)–Sc(1)–N(1), 82.91(6); N(61)–Sc(1)–N(1), 104.12(7); O(3)–Sc(1)–N(1), 156.54(6).

size of the metal center¹⁸ or its oxidation state. The coordination number of the metal center is another obvious parameter, the ligand adapting its binding mode upon the space available in the coordination sphere.

Overall, the M–O and M–Z bond distances in complexes **3–5**, **7**, and **9** are unexceptional and compare well with those observed in related group 3 metal complexes supported by phenolate-donor type ligands^{7,20} or analogous bis(trimethylsilyl)alkoxide-donor type ligands.²¹ Variations in M–O and M–Z bond distances within this series of complexes essentially reflect the difference in ionic radius between Sc, Y and La centers.¹⁸ Not enough data are available to allow for a thorough study of the effect of changing the silyl substituent and/or the donor linker. Yet, comparison between **3** and **9** shows shorter (by *ca.* 0.03–0.07 Å) M–O(THF) and M–N(SiHMe₂) bonds for the bis(naphtholate)thiophene system. This observation indicates a more electrophilic metal center in **9** than in **3**, possibly due to the weaker interaction of the metal center with the sulfur compared to the nitrogen donor.^{3f}

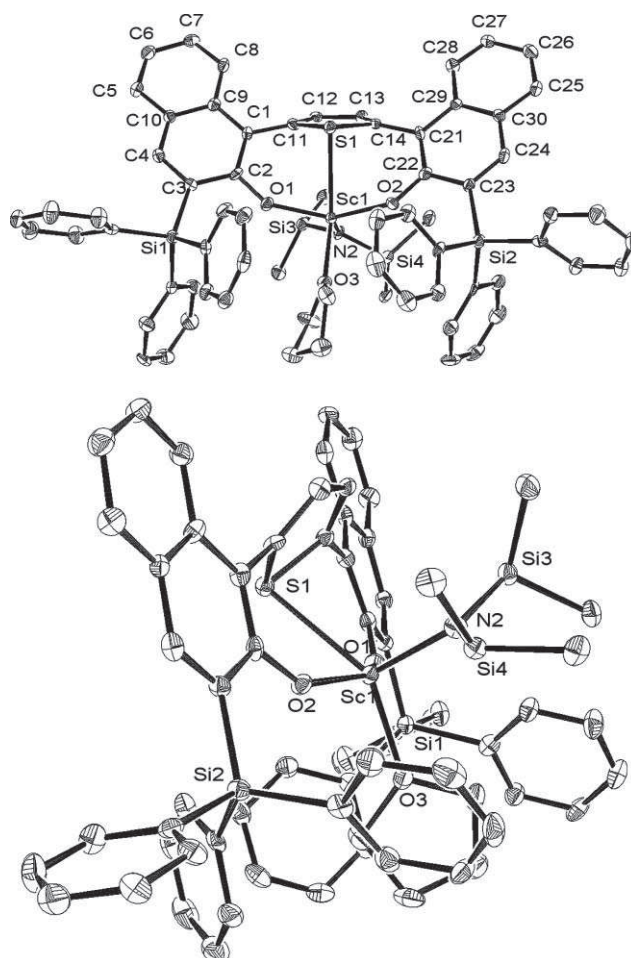
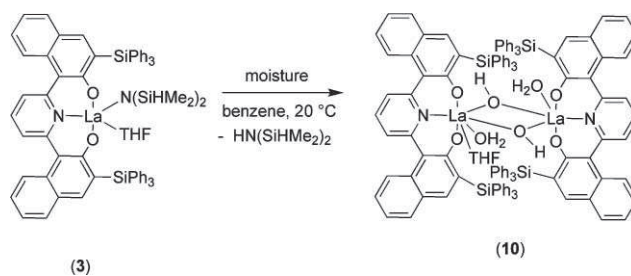


Fig. 4 ORTEP drawings of the structure of $\{\text{OSO}^{\text{SiPh}_3}\}\text{Y}-[\text{N}(\text{SiHMe}_2)_2](\text{THF})$ (**7**) (50% ellipsoid probability; H atoms are omitted for clarity). Selected bond lengths (Å) and angles (deg.): S(1)–Sc(1), 2.7758(14); Sc(1)–O(1), 1.997(3); Sc(1)–O(2), 2.008(3); Sc(1)–O(3), 2.124(3); Sc(1)–N(2), 2.027(4); O(1)–Sc(1)–O(2), 143.37(13); O(1)–Sc(1)–N(2), 106.27(15); O(2)–Sc(1)–N(2), 105.54(15); O(1)–Sc(1)–O(3), 93.18(13); O(2)–Sc(1)–O(3), 98.04(13); N(2)–Sc(1)–O(3), 101.18(14); O(1)–Sc(1)–S(1), 76.03(9); O(2)–Sc(1)–S(1), 74.91(9); N(2)–Sc(1)–S(1), 113.66(12); O(3)–Sc(1)–S(1), 145.12(10).

Upon attempting to grow single crystals of amide compound **3**, small amounts of crystals differently shaped from the main products were isolated. Though the quality of these crystals was always poor (see Table 1), X-ray diffraction revealed these crystals to be the corresponding hydroxo complex **10**, arising from adventitious hydrolysis (Scheme 4). As illustrated in Fig. 5, this compound



Scheme 4

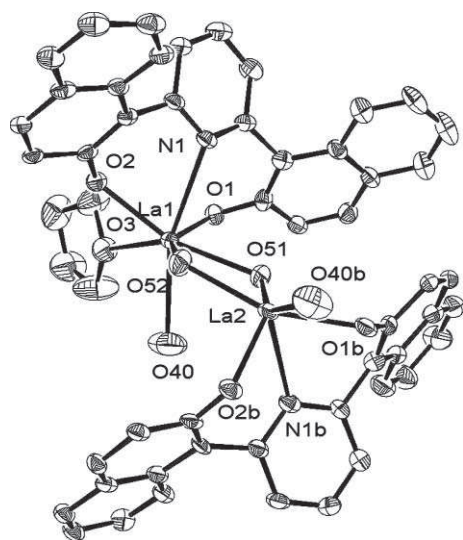


Fig. 5 ORTEP drawing of the structure of $[\{\text{ONO}^{\text{SiPh}_3}\}\text{La}(\text{THF})(\text{H}_2\text{O})(\mu\text{-OH})_2\text{La}(\text{H}_2\text{O})\{\text{ONO}^{\text{SiPh}_3}\}]$ (**10**) (50% ellipsoid probability; H atoms and SiPh_3 groups are omitted for clarity). Selected bond lengths (Å) and angles (deg.): La(1)–O(1), 2.327(4); La(1)–O(2), 2.368(4); La(1)–O(51), 2.489(4); La(1)–O(52), 2.450(5); La(1)–O(40), 2.663(5); La(1)–O(3), 2.671(4); La(1)–N(1), 2.718(4); La(2)–O(2b), 2.352(3); La(2)–O(1b), 2.362(4); La(2)–O(51), 2.383(4); La(2)–O(52), 2.430(4); La(2)–O(40b), 2.699(6); La(2)–N(1b), 2.706(5); O(1)–La(1)–O(2), 108.46(14); O(1)–La(1)–O(52), 143.63(13); O(2)–La(1)–O(52), 94.92(14); O(1)–La(1)–O(51), 81.01(14); O(2)–La(1)–O(51), 152.83(14); O(52)–La(1)–O(51), 66.51(15); O(1)–La(1)–O(40), 99.18(17); O(2)–La(1)–O(40), 127.97(18); O(52)–La(1)–O(40), 86.97(19); O(51)–La(1)–O(40), 72.95(19); O(1)–La(1)–O(3), 73.34(15); O(2)–La(1)–O(3), 70.67(14); O(52)–La(1)–O(3), 142.28(15); O(51)–La(1)–O(3), 136.05(15); O(40)–La(1)–O(3), 76.6(2); O(1)–La(1)–N(1), 72.85(14); O(2)–La(1)–N(1), 70.31(14); O(52)–La(1)–N(1), 90.20(15); O(51)–La(1)–N(1), 89.32(14); O(40)–La(1)–N(1), 161.67(19); O(3)–La(1)–N(1), 115.30(14).

adopts in the solid state a dimeric structure with μ -bridging hydroxy groups. In addition to the latter hydroxy groups, both La centers are coordinated by the tridentate $\{\text{OZO}^{\text{SiPh}_3}\}^{2-}$ ligand and one water molecule. One La center is thus six-coordinate, whereas the second one is seven-coordinate due to the presence of an additional coordinated THF molecule. The La–O bond distances (2.383(4)–2.489(4) Å) and O–La–O angles (66.5(1)–68.5(1)°) involving the bridging hydroxy groups (O(51,52)) are comparable to those observed in the other rare examples reported of dimeric hydroxy-bridged La complexes (2.385–2.421 Å and 63.05–67.92°, respectively).²² Both $\{\text{OZO}^{\text{SiPh}_3}\}^{2-}$ ligand units are coordinated with the naphtholate rings in a C_s fashion with quite similar twist angles [*i.e.*, the dihedral angle between the M–O bonds and the plane of the pyridine] of 55.0, 55.1, 55.8 and 56.3°.

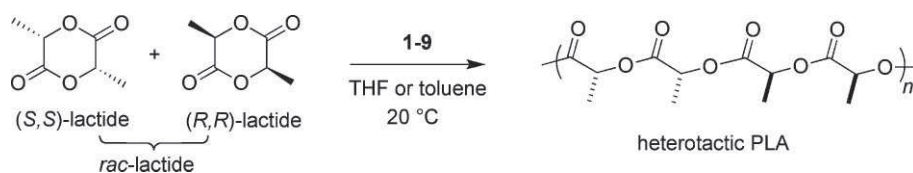
These twist angle values fall in the middle of the range observed for the parent complex **3** (49.2 and 63.3°, *vide supra*).

Preliminary studies on ring-opening polymerization of *rac*-Lactide and *rac*- β -butyrolactone

Group 3 metals and lanthanide complexes modified by ancillary ligands have received much attention in recent years for the controlled ring-opening polymerization (ROP) of cyclic esters such as lactide (LA) and, to a much lesser extent, β -butyrolactone (BBL).^{6,7,13,17} Activity ($\text{mol}_{\text{monomer}}/\text{mol}_{\text{metal}}\cdot\text{h}$), productivity ($\text{mol}_{\text{monomer}}/\text{mol}_{\text{metal}}$), degree of control/“livingness”, and stereoselectivity in the case of chiral monomers, depend crucially on ancillary ligands that define the sterics and electronics around the active metal center. Among the many systems investigated so far, a few of them have shown really valuable performances. This is notably the case of some group 3 metal complexes supported by tri- and tetradentate bis(phenolate) ligands which have been shown to induce significant heterotacticity and syndiotacticity in the ROP of *rac*-LA and *rac*- β -BBL, respectively.⁷ We were therefore interested in evaluating the catalytic performances of the new compounds **1–9** that possess a potentially active nucleophilic amido group for initiation of the ROP process and original ligand platforms.

The ability of the $\{\text{OZO}^{\text{SiR}^3}\}\text{Ln}[\text{N}(\text{SiHMe}_2)_2](\text{THF})$ complexes to promote the ROP of *rac*-LA was first examined (Scheme 5).²³ Representative results are summarized in Table 3. All complexes proved to be active at room temperature, enabling the conversion of 100–500 equiv of *rac*-LA within a few hours at most. The reactions proceeded significantly faster in toluene than in THF (compare entries 2/3, 4/9, 8/11, 16/17). This observation can probably be accounted for by the competing role of THF *vs* *rac*-LA for coordination onto the metal center. All the PLAs formed under those conditions had unimodal, although broadened molecular distributions ($M_w/M_n = 1.32\text{--}1.90$) and experimental molecular weights (determined by SEC and corrected by a factor of 0.58, due to the use of PS standards)^{24,25} quite close to the values calculated on the assumption of the growth of one macromolecular chain per metal.²⁶ For a given experiment, monitoring showed that the molecular weight increases with conversion in a perfectly linear relationship (entries 4–5, 6–8, 12–13) (Fig. 6). Also, increasing the *rac*-LA loading from 100 to 500 equiv led to proportionally higher molecular weights PLAs (at high conversion) (see, *e.g.*, entries 9/11). These data illustrate the overall good degree of control over the polymerization provided by the $\{\text{OZO}^{\text{SiR}^3}\}\text{Ln}[\text{N}(\text{SiHMe}_2)_2](\text{THF})$ systems.

Interestingly, we observed that the ROP of 500 equiv of *rac*-LA could be performed using 5 equiv of *i*PrOH (*vs* **3**), leading to a PLA with accordingly decreased molecular weight (compare entries 10–13). This experiment corresponds to a so-called “immortal” polymerization in which the added alcohol acts as a transfer agent.^{7c,27} Dormant hydroxy-end-capped polymer chains exchange

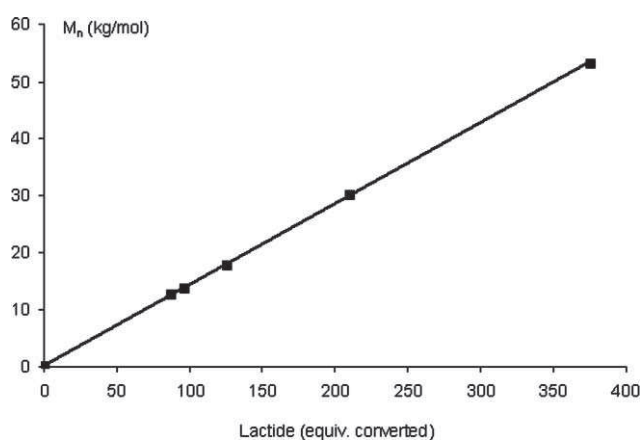


Scheme 5

Table 3 Ring-opening polymerization of *racemic* lactide promoted by {OZO^{SiR³}}Ln[N(SiHMe₂)₂](THF) complexes^a

Entry	Comp.	[LA]/[Ln]	Solvent	Time ^b /min	Conv. ^c (%)	$M_{n,calc}$ ^d /10 ³ g mol ⁻¹	$M_{n,exp}$ ^e /10 ³ g mol ⁻¹	M_w/M_n ^e	P_r ^f
1	1	100	THF	700	100	14.4	16.2	1.55	0.65
2	2	100	THF	60	71	10.2	8.9	1.32	0.90
3	2	100	toluene	3	100	14.4	10.0	1.52	0.50
4	3	100	THF	40	87	12.5	12.7	1.43	nd
5	3	100	THF	60	96	13.8	13.1	1.52	0.88
6	3	500	THF	30	25	18.0	23.1	1.39	nd
7	3	500	THF	60	42	30.3	38.2	1.55	0.87
8	3	500	THF	360	74	53.3	49.8	1.90	nd
9	3	100	toluene	2	100	14.4	17.5	1.68	0.68
10	3	500	toluene	30	41	29.5	34.2	1.51	nd
11	3	500	toluene	60	88	63.4	51.1	1.74	nd
12 ^g	3	500	toluene	30	85	12.3 ^g	10.4 ^g	1.36	nd
13 ^g	3	500	toluene	60	94	13.5 ^g	12.7 ^g	1.52	nd
14	4	100	THF	700	100	14.4	17.1	1.61	0.93
15	5	100	THF	700	100	14.4	17.3	1.52	0.84
16	6^h	100	THF	360	81	11.7	14.1	1.43	0.50
17	6^h	100	toluene	30	100	14.4	16.7	1.71	0.50
18	7	100	THF	700	100	14.4	13.1	1.42	0.66
19	8^h	100	THF	700	100	14.4	14.0	1.82	0.68
20	8^h	100	toluene	700	100	14.4	11.2	1.47	0.50
21	9	100	THF	700	100	14.4	11.6	1.51	0.75
22	9	100	toluene	700	100	14.4	12.2	1.65	0.50

^a General conditions: [*rac*-LA] = 1.0 mol L⁻¹, *T* = 20 °C. ^b Reactions times were not necessarily optimized. ^c Conversion of lactide as determined by ¹H NMR on the crude reaction mixture. ^d M_n values calculated considering one polymer chain per metal-center from the relation: $M_{n,calc} = conv \times [LA]/[Ln] \times 144$. ^e Experimental M_n and M_w/M_n values determined by GPC in THF vs. PS standards and corrected with 0.58 factor. ^f P_r is the probability of racemic linkage, as determined by ¹H NMR homodecoupling experiments. ^g Polymerizations carried out in the presence of 5 equiv of *i*PrOH vs. Ln. ^h The complex was preliminary prepared from the *in situ* reaction of the pro-ligand and tris(amido) precursor.

**Fig. 6** Relationship between M_n of PLAs and conversion of *rac*-LA (Table 3, entries 4–5, 6–8).

with the active alkoxy-type polymer chain coordinated onto Ln, enabling the growth of more (*i.e.*, 5) than one polymer chain per metal center. The polydispersity, at least similar to that observed using no *i*PrOH, and the good match between experimental and calculated molecular weights establish that this transfer reaction (exchange between dormant and active polymer chains) proceeds significantly faster than propagation.^{7e,27} Analysis by ¹H NMR spectroscopy in CDCl₃ of the low molecular weight PLAs obtained under such conditions showed clearly the existence of HOCH(CH₃)CO- (broadened quartet at δ 4.35 ppm) and C(O)OCH(CH₃)₂ (doublet at δ 1.25 ppm for the methyl groups; the resonance for the OCHMe₂ at δ *ca.* 5.1 ppm mostly overlaps with those of PLA) end-groups, thus supporting the transfer process.^{7e,25}

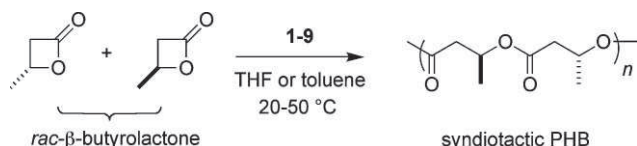
Most interestingly, homo-decoupled ¹H NMR spectroscopy showed that some of the PLAs formed with these systems had a significantly heterotactic-enriched microstructure. The probability of racemic linkage (P_r) ranged from 0.50 (atactic) up to 0.93. As we observed with tetradentate bis(phenolato)-lanthanide systems,^{7b-e} the stereoselectivity strongly depended on the nature of the solvent: almost all the PLAs produced in toluene had an atactic microstructure whereas those obtained in THF were almost always heterotactic. The degree of heterotacticity was also quite different among the series of compounds **1–9**, and appears to be affected by the nature of the metal center (Sc, Y, La), the central linker in the ligand framework (pyridine, thiophene), and the *ortho*-silyl substituent (SiPh₃, SiMe₂*t*Bu) as well. The bis(naphtholate)-thiophene framework is less efficient than that based on 2,6-pyridine; one can speculate that the [anticipated] weaker interaction of the soft S (as compared to the harder N) atom induces a larger flexibility of the ligand and, as a result, a less sterically rigid coordination sphere around the active metal center. Within the series of {ONO^{SiMe₂*t*Bu}}–Ln complexes **4–6**, the tacticity decreases with increasing ionic radius¹⁸ (metal, P_r : Sc, 0.93; Y, 0.84; La, 0.50). The same trend was observed with tetradentate bis(phenolato)-lanthanide systems,^{7b-e} and was proposed to reflect a better contribution of sterically constrained metal centers on the chain-end stereocontrol.²⁸ The aforementioned “ionic radius/heterotacticity” trend is, however, not observed within the series of {ONO^{SiPh₃}}–Ln complexes **1–3**, since the smaller Sc led to a modest P_r value of 0.65 whereas the small Y and large La afforded about the same high heterotacticity (P_r = 0.88–0.90).

The less reactive *rac*-BBL could also be polymerized to afford syndiotactic-enriched poly(3-hydroxybutyrate)s (PHBs) (Scheme 6). Representative results are summarized in Table 4.

Table 4 Ring-opening polymerization of *racemic* β -butyrolactone promoted by $\{\text{OZO}^{\text{SiR}^3}\}\text{Ln}[\text{N}(\text{SiHMe}_2)_2](\text{THF})$ complexes^a

Entry	Comp.	[BBL]/[Ln]	Solvent	Time ^b /min	Conv. ^c (%)	$M_{n,\text{calc}}$ ^d /10 ³ g mol ⁻¹	$M_{n,\text{exp}}$ ^e /10 ³ g mol ⁻¹	M_w/M_n ^e	P_r ^f
1 ^g	1	100	toluene	1000	30	2.2	5.9	1.69	0.48
2 ^{g,h}	1	100	toluene	1000	62	5.3	7.1	1.32	0.48
3	2	100	toluene	300	100	8.6	40.7	1.12	0.76
4	2	300	THF	700	30	7.7	18.4	1.41	0.53
5	2	100	THF	300	73	6.3	31.3	1.17	0.57
6	2	300	toluene	700	70	18.1	20.3	1.29	0.78
7 ^{g,h}	2	100	toluene	30	100	8.6	17.8	1.32	0.87
8	3	100	THF	100	80	6.9	11.1	1.25	0.53
9	3	100	toluene	2	24	2.1	2.6	1.12	0.86
10	3	100	toluene	15	62	5.3	7.0	1.38	nd
11 ^{g,h}	7	100	toluene	1000	40	3.4	3.2	1.45	0.60
12	8	100	THF	1000	20	5.2	14.2	1.35	0.52
13	8	100	toluene	1000	30	7.7	11.0	1.22	0.67
14	9	300	THF	1000	100	25.8	23.5	1.35	0.46
15	9	300	toluene	360	92	23.7	18.6	1.38	0.55

^a General conditions unless otherwise stated: $[\text{rac-BBL}] = 3.0 \text{ mol L}^{-1}$, $T = 20^\circ\text{C}$. ^b Reactions times were not necessarily optimized. ^c Conversion of lactide as determined by ^1H NMR on the crude reaction mixture. ^d M_n values calculated considering one polymer chain per metal-center from the relation: $M_{n,\text{calc}} = \text{conv} \times [\text{BBL}]/[\text{Ln}] \times 74$. ^e Experimental M_n (uncorrected) and M_w/M_n values determined by GPC in THF vs. PS standards. ^f P_r is the probability of racemic linkage, as determined by ^{13}C NMR. ^g Reaction carried out at 50°C . ^h Polymerizations carried out in the presence of 1 equiv of *i*PrOH vs. Ln.

**Scheme 6**

At first, it must be noted that compounds **4–6** did not show any activity under the conditions investigated (THF, toluene, 20–50 °C). Apparently, the inertness of this series of complexes seems to arise from the presence of SiMe_2tBu *ortho*-substituents, although the exact reason still remains obscure. The $\{\text{OZO}^{\text{SiPh}_3}\}\text{-Ln}$ compounds **1–3** and **7–8** are active in the ROP of *rac*-BBL at room temperature, but an increase of the reaction temperature to 50°C did prove useful in some cases to reduce the reaction time. This was particularly the case for scandium complexes **1** and **7**, which are quite sluggish (entries 1, 2, 11). In those cases, the addition of 1 equiv of *i*PrOH (vs Ln), to generate *in situ* the corresponding $\{\text{OZO}^{\text{SiPh}_3}\}\text{Sc-isopropoxide}$ species,^{7b-d} enabled faster reactions, suggesting a relatively slow initiation with amido precursors (compare entries 1/2). Lanthanum complexes **3** and **9** showed the highest reaction rates. Similarly to the ROP of *rac*-LA, the ROP of *rac*-BBL with these systems proceeded faster in toluene than in THF.

Most of the resulting PHBs had experimental molecular weights (determined by SEC, uncorrected) in the range $4.1\text{--}28.1 \times 10^3 \text{ g mol}^{-1}$, which are in good agreement with the theoretical values [calculated assuming the growth of one polymer chain per metal center].²⁹ Molecular weights larger than those calculated were observed in some cases (entries 3, 5, 7, 12), apparently when low $[\text{rac-BBL}]/[\text{Ln}]$ ratios were used; exact reasons for these discrepancies remain unclear at this time but one may speculate that the initiation efficiency is low under such conditions. The molecular weight distributions were unimodal and somewhat narrower ($M_w/M_n = 1.12\text{--}1.69$) than those observed for PLAs, indicative of the controlled character of the polymerizations. Detailed ^{13}C NMR analysis^{7f} revealed that some PHBs had a

significantly syndiotactic-enriched microstructure, with P_r values^{7f} ranging from 0.48 (*i.e.*, atactic) up to 0.87. As exemplified for complexes **2**, **3** and **9**, the use of toluene as solvent led always to higher stereoselectivities than with THF; *i.e.*, the opposite trend than that observed for the ROP of *rac*-LA (*vide supra*) but a trend consistent with our previous observations in the ROP of *rac*-BBL using tetradentate bis(phenolate)-Ln systems.^{7d,f} In line with the results for the ROP of *rac*-LA, the bis(naphtholate)-thiophene framework $\{\text{OSO}^{\text{SiPh}_3}\}^{2-}$ led to lower stereoselectivities (**7-9**, $P_r = 0.55\text{--}0.67$) than that based on 2,6-pyridine $\{\text{ONO}^{\text{SiPh}_3}\}^{2-}$, especially the Y and La complexes (**2**, **3**, $P_r = 0.76\text{--}0.87$ and 0.86, respectively). The latter levels of syndiotacticity are just below those we achieved with tetradentate bis(phenolate)-Ln systems (the most stereoselective systems reported to date; $P_r =$ up to 0.94),^{7d,f} and range among the highest reported thus far for the ROP of *rac*-BBL.

Conclusions

In conclusion, we have readily prepared in high yields a series of scandium, yttrium and lanthanum amido complexes supported by tridentate bis(*ortho*-silyl-substituted naphtholate)-donor ligands, *via* the reaction of the corresponding pro-ligand $\{\text{OZO}^{\text{SiR}^3}\}\text{H}_2$ and $\text{Ln}[\text{N}(\text{SiHMe}_2)_2]_3(\text{THF})_n$ precursor. Those complexes all adopt a C_s -symmetric ground state structure in the solid state, as observed for compounds **1–3** and **7–9**, and in toluene solution as well.

Compounds **1–9** are single-site initiators for the ROP of *rac*-LA at 20°C , affording PLAs with relatively narrow polydispersities and molecular weights in good agreement with calculated values. Atactic polymers are formed in toluene but, when carried out in THF, the polymerizations afforded heterotactic-enriched PLAs (P_r up to 0.93). Immortal polymerization, with good control over the number and molecular weight of polymer chains, can be performed upon addition of isopropanol as a transfer agent. Compounds **1–3** and **7–9**, having *o*- SiPh_3 substituents on the naphtholate rings, are also active for the ROP of *rac*-BBL at $20\text{--}50^\circ\text{C}$, to form syndiotactic-enriched PHBs (P_r up to 0.87) when using toluene as the solvent, whereas essentially atactic

2H, Haro), 7.31 (d, $^3J = 7.7$, 2H, H^{ar}), 7.29–7.19 (m, 18H, Haro), 7.17 (m, 2H, Haro), 6.98 (t, $^3J = 7.7$, 1H, H^{3p}), 4.29 (sept, $^3J = 2.8$, 2H, $SiHMe$), 3.07 (br m, 4H, $\alpha-CH_2$, THF), 1.07 (br m, 4H, $\beta-CH_2$, THF), –0.11 (d, $^3J = 2.8$, 12H, $SiHMe_2$). $^{13}C\{^1H\}$ NMR (125 MHz, benzene- d_6 , 298 K): δ 162.1, 156.6, 144.3, 138.5, 137.0, 136.9, 132.6, 129.3, 129.2, 128.3, 128.0, 127.9, 127.8, 127.3, 123.8, 121.9, 118.3 (Caro), 68.3 ($\alpha-CH_2$, THF), 24.9 ($\beta-CH_2$, THF), –2.5 ($SiHMe_2$). Anal. calcd. for $C_{69}H_{65}LaN_2O_3Si_4$: C, 67.85; H, 5.36; N, 2.29. Found: C, 67.3; H, 5.4; N, 2.3.

$\{ONO^{SiBuMe_2}\}_3Sc[N(SiHMe_2)_2](THF)$ (**4**)

This compound was prepared following the same procedure as that described above for **1**, starting from $\{ONO^{SiBuMe_2}\}_3H_2$ (0.046 g, 0.090 mmol) and $Sc[N(SiHMe_2)_2](THF)$ (0.040 g, 0.090 mmol) in benzene (5 mL). Compound **4** was obtained as a pale yellow microcrystalline material (0.067 g, 72%). Crystals of **4** suitable for X-ray diffraction analysis were prepared by prolonged crystallization from a concentrated benzene solution at room temperature. 1H NMR (500 MHz, benzene- d_6 , 298 K): δ 8.36 (s, 2H 4), 8.01 (br d, $^3J = 8.2$, 2H, H^5), 7.86 (br d, $^3J = 7.9$, 2H, H^8), 7.39 (br t, $^3J = 7.9$, 2H, H^7), 7.29 (m, 4H, H^{6+2p}), 6.92 (br t, $^3J = 7.7$, 1H, H^{3p}), 4.63 (br m, 2H, $SiHMe$), 4.49 (br m, 4H, $\alpha-CH_2$, THF), 1.73 (br m, 4H, $\beta-CH_2$, THF), 1.27 (s, 18H, $SiMe_2tBu$), 0.71 (s, 6H, $SiMeMerBu$), 0.68 (s, 6H, $SiMeMerBu$), –0.20 (br s, 12H, $SiHMe_2$). $^{13}C\{^1H\}$ NMR (125 MHz, benzene- d_6 , 298 K): δ 163.7, 140.6, 136.6, 135.4, 128.7, 128.3, 128.1, 128.0, 127.9, 126.97, 123.8, 122.2 (Caro), 71.3 ($\alpha-CH_2$, THF), 27.6 ($C(CH_3)_3$), 25.2 ($\beta-CH_2$, THF), 17.9 ($C(CH_3)_3$), 2.8 ($SiMe_2tBu$), 2.2 ($SiHMe_2$). VT 1H NMR: 1H NMR (500 MHz, toluene- d_8 , 338 K): δ 8.17 (s, 2H 4), 7.87 (br d, $^3J = 8.3$, 2H 5), 7.70 (br d, $^3J = 7.9$, 2H 8), 7.26 (m, 4H $^{6+2p}$), 7.16 (br t, $^3J = 7.9$, 2H 7), 7.05 (br m, 1H 3p), 4.51 (br m, 2H, $SiHMe$), 4.34 (br m, 4H, $\alpha-CH_2$, THF), 1.72 (br m, 4H, $\beta-CH_2$, THF), 1.13 (s, 18H, $SiMe_2tBu$), 0.58 (s, 12H, $SiMe_2tBu$), –0.31 (s, 12H, $SiHMe_2$). 1H NMR (500 MHz, toluene- d_8 , 313 K): δ 8.20 (s, 2H 4), 7.88 (br d, $^3J = 8.2$, 2H 5), 7.71 (br d, $^3J = 7.9$, 2H 8), 7.27 (br t, $^3J = 7.9$, 2H 7), 7.22 (br d, $^3J = 7.7$, 2H 2p), 7.17 (br t, $^3J = 8.2$, 2H 6), 6.98 (br t, $^3J = 7.7$, 1H 3p), 4.50 (br m, 2H, $SiHMe$), 4.33 (br m, 4H, $\alpha-CH_2$, THF), 1.71 (br m, 4H, $\beta-CH_2$, THF), 1.51 (s, 18H, $SiMe_2tBu$), 0.59 (s, 12H, $SiMe_2tBu$), –0.32 (s, 12H, $SiHMe_2$). 1H NMR (500 MHz, toluene- d_8 , 298 K): δ 8.21 (s, 2H 4), 7.89 (br d, $^3J = 8.3$, 2H 5), 7.72 (br d, $^3J = 7.7$, 2H 8), 7.27 (br t, $^3J = 7.7$, 2H 7), 7.19 (m, 4H $^{6+2p}$), 6.94 (br t, $^3J = 7.9$, 1H 3p), 4.49 (br s, 2H, $SiHMe$), 4.40 (m, 4H, $\alpha-CH_2$, THF), 1.75 (m, 4H, $\beta-CH_2$, THF), 1.16 (s, 18H, $SiMe_2tBu$), 0.16 (br s, 12H, $SiMe_2tBu$), –0.30 (br s, 12H, $SiHMe_2$). 1H NMR (500 MHz, toluene- d_8 , 273 K): δ 8.24 (s, 2H 4), 7.90 (br d, $^3J = 8.3$, 2H 5), 7.73 (br d, $^3J = 7.7$, 2H 8), 7.29 (br t, $^3J = 7.7$, 2H 7), 7.20 (br t, $^3J = 8.3$, 2H 6), 7.17 (m, 2H 2p), 6.86 (br t, $^3J = 7.7$, 1H 3p), 4.48 (br m, 2H, $SiHMe$ + 4H, $\alpha-CH_2$, THF), 1.78 (br m, 4H, $\beta-CH_2$, THF), 1.19 (s, 18H, $SiMe_2tBu$), 0.63 (s, 6H, $SiMeMerBu$), 0.59 (s, 6H, $SiMeMerBu$), –0.32 (s, 12H, $SiHMe_2$). 1H NMR (500 MHz, toluene- d_8 , 223 K): δ 8.28 (s, 2H 4), 7.93 (d, $^3J = 8.6$, 2H 5), 7.75 (d, $^3J = 8.6$, 2H 8), 7.80 (m, 2H 6), 7.22 (m, 2H 7), 7.11 (m, 2H 2p), 6.74 (t, $^3J = 7.8$, 1H 3p), 4.52 (sept, $^3J = 3.0$, 2H, $SiHMe$), 4.45 (m, 4H, $\alpha-CH_2$, THF), 1.65 (m, 4H, $\beta-CH_2$, THF), 1.22 (s, 18H, $SiMe_2tBu$), 0.65 (s, 6H, $SiMeMerBu$), 0.62 (s, 6H, $SiMeMerBu$), –0.30 (d, $J = 3.0$, 12H, $SiHMe_2$). Anal. calcd. for $C_{45}H_{65}N_2O_3Si_4$: C, 64.40; H, 7.81; N, 3.34. Found: C, 63.8; H, 8.2; N, 3.4.

$\{ONO^{SiBuMe_2}\}_3Y[N(SiHMe_2)_2](THF)$ (**5**)

This compound was prepared following the same procedure as that described above for **1**, starting from $\{ONO^{SiBuMe_2}\}_3H_2$ (0.063 g, 0.110 mmol) and $Y[N(SiHMe_2)_2](THF)$ (0.060 g, 0.110 mmol) in benzene (5 mL). Compound **5** was obtained as a pale yellow microcrystalline material (0.083 g, 85%). Crystals of **5** suitable for X-ray diffraction analysis were prepared by prolonged crystallization from a concentrated benzene solution at room temperature. 1H NMR (500 MHz, benzene- d_6 , 298 K): δ 8.34 (s, 2H, H^4), 7.86 (d, $^3J = 7.5$, 2H, H^5), 7.79 (br d, $^3J = 8.0$, 2H, H^8), 7.36 (t, $^3J = 8.0$, 2H, H^7), 7.28 (m, 2H, H^6), 7.19 (br d, $^3J = 7.7$, 2H, H^{2p}), 6.97 (t, $^3J = 7.7$, 1H, H^{3p}), 4.76 (br m, 2H, $SiHMe$), 4.01 (br m, 4H, $\alpha-CH_2$, THF), 1.31 (br m, 4H, $\beta-CH_2$, THF + 18H, $SiMe_2tBu$), 0.78 (br s, 6H, $SiMeMerBu$), 0.71 (br s, 6H, $SiMeMerBu$), 0.03 (br s, 12H, $SiHMe_2$). $^{13}C\{^1H\}$ NMR (125 MHz, benzene- d_6 , 298 K): δ 163.6, 140.4, 136.9, 136.0, 130.5, 128.8, 128.3, 128.1, 126.9, 126.7, 123.3, 121.7 (Caro), 70.9 ($\alpha-CH_2$, THF), 27.7 ($C(CH_3)_3$), 24.9 ($\beta-CH_2$, THF), 17.9 ($C(CH_3)_3$), 3.0 ($SiMe_2tBu$), 2.8 ($SiHMe_2$). VT 1H NMR: 1H NMR (500 MHz, toluene- d_8 , 338 K): δ 8.16 (s, 2H 4), 7.70 (dd, $^3J = 7.9$ and 1.5, 2H 5), 7.65 (br dd, $^3J = 8.3$ and 1.1, 2H 8), 7.22 (ddd, $^{3,3,4}J = 8.3$, 6.8 and 1.5, 2H 7), 7.19 (dd, $^3J = 7.9$ and 0.6, 2H 2p), 7.12 (ddd, $^{3,3,4}J = 7.9$, 6.8 and 1.1, 2H 6), 7.11 (t, $^3J = 7.9$, 1H 3p), 4.57 (br m, 2H, $SiHMe$), 3.96 (br m, 4H, $\alpha-CH_2$, THF), 1.44 (br m, 4H, $\beta-CH_2$, THF), 1.16 (s, 18H, $SiMe_2tBu$), 0.60 (s, 12H, $SiMe_2tBu$), –0.15 (br d, $J = 2.1$, 12H, $SiHMe_2$). 1H NMR (500 MHz, toluene- d_8 , 313 K): δ 8.18 (s, 2H 4), 7.71 (dd, $^3J = 7.9$, 1.3, 2H 5), 7.63 (br dd, $^3J = 8.1$ and 1.1, 2H 8), 7.23 (ddd, $^{3,3,4}J = 8.1$, 6.6, and 1.3, 2H 7), 7.14 (ddd, $^{3,3,4}J = 7.9$, 6.6, and 1.1, 2H 6), 7.13 (m, 2H 2p), 7.05 (br m, 1H 3p), 4.64 (br m, 2H, $SiHMe$), 3.92 (br m, 4H, $\alpha-CH_2$, THF), 1.32 (br m, 4H, $\beta-CH_2$, THF), 1.19 (s, 18H, $SiMe_2tBu$), 0.67 (br s, 6H, $SiMeMerBu$), 0.61 (br s, 6H, $SiMeMerBu$), –0.05 (br s, 12H, $SiHMe_2$). 1H NMR (500 MHz, toluene- d_8 , 296 K): δ 8.19 (s, 2H 4), 7.72 (dd, $^3J = 7.7$ and 1.5, 2H 5), 7.64 (br s, 2H 8), 7.24 (ddd, $^{3,3,4}J = 8.3$, 6.8, and 1.5, 2H 7), 7.15 (ddd, $^{3,3,4}J = 1.1$, 6.8, and 7.7, 2H 6), 7.11 (br m, 2H 2p), 7.06 (br m, 1H 3p), 4.66 (br m, 2H, $SiHMe$), 3.91 (br m, 4H, $\alpha-CH_2$, THF), 1.31 (br m, 4H, $\beta-CH_2$, THF), 1.20 (s, 18H, $SiMe_2tBu$), 0.70 (br s, 6H, $SiMeMerBu$), 0.62 (br s, 6H, $SiMeMerBu$), –0.01 (br s, 12H, $SiHMe_2$). 1H NMR (500 MHz, toluene- d_8 , 263 K): δ 8.23 (s, 2H 4), 7.73 (br d, $^3J = 7.9$, 2H 5), 7.73 (br m, 2H 8), 7.26 (br m, 2H 7), 7.16 (br m, 4H $^{6+2p}$), 6.88 (br tr, $^3J = 7.9$, 1H 3p), 4.51 (br m, 2H, $SiHMe$), 3.69 (br m, 4H, $\alpha-CH_2$, THF), 1.33 (br m, 4H, $\beta-CH_2$, THF), 1.24 (s, 18H, $SiMe_2tBu$), 0.63 (br s, 12H, $SiMe_2tBu$), –0.27 (br s, 12H, $SiHMe_2$). 1H NMR (500 MHz, toluene- d_8 , 233 K): δ 8.27 (s, 2H 4), 7.77 (m, 3H), 7.53 (m, 1H), 7.27 (m, 3H), 7.11 (br s, 2H), 6.78 (m, 2H), 4.53 (br m, 2H, $SiHMe$), 4.15 (br m, 2H, $\alpha-CH_2$, THF), 3.66 (br m, 2H, $\alpha-CH_2$, THF), 1.35 (br m, 4H, $\beta-CH_2$, THF), 1.25 (s, 18H, $SiMe_2tBu$), 0.64 (br s, 6H, $SiMeMerBu$), 0.62 (br s, 6H, $SiMeMerBu$), –0.24 (br s, 12H, $SiHMe_2$). Anal. calcd. for $C_{45}H_{65}N_2O_3Si_4Y$: C, 61.19; H, 7.42; N, 3.17. Found: C, 60.8; H, 8.1; N, 3.0.

NMR-scale generation of $\{ONO^{SiBuMe_2}\}_3La[N(SiHMe_2)_2](THF)$ (**6**)

Complex **6** was generated *in situ* from the 1:1 reaction of $\{ONO^{SiBuMe_2}\}_3H_2$ with $La[N(SiHMe_2)_2](THF)_2$. The 1H NMR spectrum of the reaction mixture was quite complicated and could not be unambiguously assigned.

{OSO^{SiPh₃}}Sc[N(SiHMe₂)₂](THF) (7)

This compound was prepared following the same procedure as that described above for **1**, starting from {OSO^{SiPh₃}}H₂ (0.068 g, 0.090 mmol) and Sc[N(SiHMe₂)₂]₃(THF) (0.040 g, 0.090 mmol) in benzene (5 mL). Compound **7** was obtained as a pale yellow microcrystalline powder (0.076 g, 75%). Crystals of **7** suitable for X-ray diffraction analysis were prepared by prolonged crystallization from a concentrated benzene solution at room temperature. ¹H NMR (500 MHz, benzene-*d*₆, 298 K): δ 8.35 (d, ³*J* = 8.4, 2H, Haro) 8.06 (s, 2H, H⁴), 7.81–7.83 (m, 12H, Haro), 7.53 (t, ³*J* = 7.6, 2H, H⁷), 7.49 (s, 2H, thiophene), 7.43 (d, ³*J* = 7.6, 2H, H⁸), 7.26–7.30 (m, 18H, Haro), 7.15 (t, ³*J* = 7.7, 2H, H⁶), 4.34 (sept, ³*J* = 2.9, 2H, SiHMe), 2.82 (m, 4H, α-CH₂, THF), 0.69 (m, 4H, β-CH₂, THF), 0.05 (d, ³*J* = 3.2, 12H, SiHMe₂). ¹³C{¹H} NMR (125 MHz, benzene-*d*₆, 298 K): δ 168.8, 143.7, 141.4, 136.6, 136.5, 134.9, 133.5, 129.2, 129.1, 128.3, 128.1, 128.0, 127.6, 125.5, 123.4, 122.3, 115.4 (Caro), 71.6 (α-CH₂, THF), 24.4 (β-CH₂, THF), 2.8 (SiHMe₂). Anal. calcd. for C₆₈H₆₄NO₃SScSi₄: C, 72.11; H, 5.70; N, 1.24. Found: C, 71.8; H, 6.1; N, 1.2.

{OSO^{SiPh₃}}Y[N(SiHMe₂)₂](THF) (8)

This compound was prepared following the same procedure as that described above for **1**, starting from {OSO^{SiPh₃}}H₂ (0.064 g, 0.070 mmol) and Y[N(SiHMe₂)₂]₃(THF) (0.040 g, 0.070 mmol) in benzene (5 mL). Compound **8** was obtained as a pale yellow microcrystalline powder (0.065 g, 81%). ¹H NMR (500 MHz, benzene-*d*₆, 298 K): δ 8.08 (s, 2H, H⁴), 7.94 (d, ³*J* = 8.4, 2H, Haro), 7.85–7.87 (m, 12H, Haro), 7.55 (s, 2H, thiophene), 7.49 (t, ³*J* = 7.8, 2H), 7.42 (d, ³*J* = 7.8, 2H, Haro), 7.27–7.31 (m, 18H, Haro), 7.13 (t, ³*J* = 7.8, 2H), 4.55 (sept, ³*J* = 2.9, 2H, SiHMe), 2.85 (m, 4H, α-CH₂, THF), 0.68 (m, 4H, β-CH₂, THF), 0.14 (d, ³*J* = 2.9, 12H, SiHMe). ¹³C{¹H} NMR (125 MHz, benzene-*d*₆, 298 K): δ 171.8, 149.6, 144.2, 136.8, 136.7, 136.4, 135.6, 132.4, 129.2, 128.4, 128.1, 127.6, 126.9, 126.6, 122.6, 121.8, 112.1 (Caro), 70.6 (α-CH₂, THF), 24.4 (β-CH₂, THF), 3.4 (SiHMe₂). Anal. calcd. for C₆₈H₆₄NO₃SSi₄Y: C, 69.42; H, 5.48; N, 1.19. Found: C, 68.8; H, 5.37; N, 1.2.

{OSO^{SiPh₃}}La[N(SiHMe₂)₂](THF) (9)

This compound was prepared following the same procedure as that described above for **1**, starting from {OSO^{SiPh₃}}H₂ (0.165 g, 0.180 mmol) and La[N(SiHMe₂)₂]₃(THF)₂ (0.127 g, 0.180 mmol) in benzene (10 mL). Compound **9** was obtained as a pale yellow microcrystalline powder (0.224 g, 96%). Crystals of **9** suitable for X-ray diffraction analysis were prepared by prolonged crystallization from a benzene solution at room temperature. ¹H NMR (500 MHz, benzene-*d*₆, 298 K): δ 8.08 (s, 2H, H⁴), 7.94 (d, ³*J* = 8.3 Hz, 2H, Haro), 7.89 (m, 12H, Haro), 7.52 (s, 2H, thiophene), 7.49 (m, 2H, Haro), 7.42 (d, ³*J* = 8.3, 2H, Haro), 7.33 (m, 18H, Haro), 7.13 (m, 2H, Haro), 4.55 (sept, ³*J* = 2.8, 2H, SiHMe), 2.70 (br m, 4H, α-CH₂, THF), 0.76 (br m, 4H, β-CH₂, THF), 0.19 (d, ³*J* = 2.8, 12H, SiHMe₂). ¹³C{¹H} NMR (125 MHz, benzene-*d*₆, 298 K): δ 173.0, 151.8, 143.8, 136.6, 136.5, 136.1, 132.0, 129.1, 129.0, 128.1, 127.9, 126.9, 126.6, 122.7, 121.5, 111.6 (Caro), 69.1 (α-CH₂, THF), 24.5 (β-CH₂, THF), 3.1 (SiHMe₂). Anal. calcd. for C₆₈H₆₄LaNO₃SSi₄: C, 66.59; H, 5.26; N, 1.14. Found: C, 66.8; H, 5.57; N, 1.0.

Crystal structure determination of complexes 3–5, 7, 9 and 10

Suitable crystals for X-ray diffraction analysis of **3–5**, **7**, **9** and **10** were obtained by crystallization of purified products from concentrated benzene solutions (see the Experimental section and body text). Diffraction data were collected at 100 K using a Bruker APEX CCD diffractometer with graphite-monochromated Mo-Kα radiation (λ = 0.71073 Å). A combination of ω and φ scans was carried out to obtain at least a unique data set. The crystal structures were solved by direct methods using the SIR97 program,³⁰ remaining atoms were located from difference Fourier synthesis followed by full-matrix least-squares refinement based on *F*² (programs SHELXS-97 and SHELXL-97)³¹ with the aid of the WINGX program.³² Many hydrogen atoms could be found from the Fourier difference analysis. Carbon- and oxygen-bound hydrogen atoms were placed at calculated positions and forced to ride on the attached atom. The hydrogen atom contributions were calculated but not refined. All non-hydrogen atoms were refined with anisotropic displacement parameters. The locations of the largest peaks in the final difference Fourier map calculation as well as the magnitude of the residual electron densities were of no chemical significance. In **4** and **5**, one *t*Bu group and one Si(2)-Me group were found to be disordered and accordingly modelled. Crystals of **10** were found to contain lattice disordered solvent molecules (benzene), all of which could not be satisfactorily modelled and were removed using the SQUEEZE procedure³³ implemented in the PLATON package.³⁴ Crystal data and details of data collection and structure refinement for the different compounds are given in Table 1. Crystallographic data are also available as cif files (see the ESI†).

Typical procedure for *rac*-LA and *rac*-BBL polymerization

In a glovebox, a Schlenk flask was charged with a solution of complex **1** (7.0 mg, 5.8 μmol) in THF or toluene (0.20–0.60 mL). To this solution, the monomer (0.58 mmol, 100 equiv vs. La; *rac*-LA: 82.6 mg, *rac*-BBL: 49.3 mg) was rapidly added under vigorous stirring at 20 °C. Small aliquots of the reaction mixture were periodically sampled with pipette for determining the conversion by ¹H NMR spectrometry. After the desired time, the reaction was quenched by adding acidic methanol (*ca.* 1 mL of a 1.2M HCl solution in CH₃OH) and the polymer was precipitated with excess methanol (*ca.* 3 mL). The supernatant solution was removed with pipette and the polymer was dried under vacuum to constant weight.

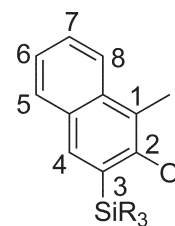
Acknowledgements

This work was financially supported by Agence Nationale de la Recherche (grant ANR-06-BLAN-0213). JFC gratefully thanks the Institut Universitaire de France for a Junior IUF fellowship (2005–2009).

References

- For reviews on alkoxo- and aryloxo-metal chemistry, see: (a) D. C. Bradley, R. M. Mehrotra, I. P. Rothwell, A. Singh *Alkoxo and Aryloxo Derivatives of Metals*, Academic Press, London, 2001; (b) R. M. Mehrotra and A. Singh, *Prog. Inorg. Chem.*, 1997, **46**, 239; (c) R. C. Mehrotra, A. Singh and U. M. Tripathi, *Chem. Rev.*, 1991, **91**, 1287.

- 2 For selected leading references, see: (a) J. Tian and G. W. Coates, *Angew. Chem., Int. Ed.*, 2000, **39**, 3626; (b) P. D. Hustad, J. Tian and G. W. Coates, *J. Am. Chem. Soc.*, 2002, **124**, 3614; (c) S. Reinartz, A. F. Mason, E. B. Lobkovsky and G. W. Coates, *Organometallics*, 2003, **22**, 2542; (d) A. F. Mason and G. W. Coates, *J. Am. Chem. Soc.*, 2004, **126**, 10798; (e) A. F. Mason and G. W. Coates, *J. Am. Chem. Soc.*, 2004, **126**, 16326; (f) J. Saito, M. Mitani, J. Mohri, Y. Yoshida, S. Matsui, S. Ishii, S. Kojoh, N. Kashiwa and T. Fujita, *Angew. Chem., Int. Ed.*, 2001, **40**, 2918; (g) S. Matsui, M. Mitani, J. Saito, Y. Tohi, H. Makio, N. Matsukawa, Y. Takagi, K. Tsuru, M. Nitabaru, T. Nakano, H. Tanaka, N. Kashiwa and T. Fujita, *J. Am. Chem. Soc.*, 2001, **123**, 6847; (h) T. Matsugi and F. Fujita, *Chem. Soc. Rev.*, 2008, **37**, 1264.
- 3 For selected leading references, see: (a) R. M. Gauvin, J. A. Osborn and J. Kress, *Organometallics*, 2000, **19**, 2944; (b) K. Takaoki and T. Miyatake, *Macromol. Symp.*, 2000, **157**, 251; (c) Y. Nakayama, K. Watanabe, N. Ueyama, A. Nakamura, A. Harada and J. Okuda, *Organometallics*, 2000, **19**, 2498; (d) M. C. W. Chan, K. H. Tam, Y. L. Pui and N. Y. Zhu, *J. Chem. Soc., Dalton Trans.*, 2002, 3085; (e) M. C. W. Chan, K. H. Tam, N. Y. Zhu, P. Chiu and S. Matsui, *Organometallics*, 2006, **25**, 785; (f) T. Agapie, L. M. Henling, A. G. DiPasquale, A. L. Rheingold and J. E. Bercaw, *Organometallics*, 2008, **27**, 6245.
- 4 For selected leading references, see: (a) E. Y. Tshuva, I. Goldberg, M. Kol, H. Weitman and Z. Goldschmidt, *Chem. Commun.*, 2000, 379; (b) E. Y. Tshuva, I. Goldberg and M. Kol, *J. Am. Chem. Soc.*, 2000, **122**, 10706; (c) E. Y. Tshuva, I. Goldberg, M. Kol and Z. Goldschmidt, *Chem. Commun.*, 2001, 2120; (d) E. Y. Tshuva, I. Goldberg and M. Kol, *J. Am. Chem. Soc.*, 2001, **123**, 3621; (e) E. Y. Tshuva, I. Goldberg, M. Kol and Z. Goldschmidt, *Organometallics*, 2001, **20**, 3017; (f) E. Y. Tshuva, S. Groysman, I. Goldberg, M. Kol and Z. Goldschmidt, *Organometallics*, 2002, **21**, 662; (g) S. Groysman, E. Y. Tshuva, I. Goldberg, M. Kol, Z. Goldschmidt and M. Shuster, *Organometallics*, 2004, **23**, 5291; (h) S. Segal, I. Goldberg and M. Kol, *Organometallics*, 2005, **24**, 200; (i) C. Capacchione, A. Proto, H. Ebeling, R. Mulhaupt, K. Moller, T. P. Spaniol and J. Okuda, *J. Am. Chem. Soc.*, 2003, **125**, 4964; (j) C. Capacchione, F. De Carlo, C. Zannoni, J. Okuda and A. Proto, *Macromolecules*, 2004, **37**, 8918; (k) B. Lian, T. P. Spaniol and J. Okuda, *Organometallics*, 2007, **26**, 6653; (l) G. J. M. Meppelder, K. Beckerle, R. Manivannan and J. Okuda, *Chem.-Asian J.*, 2008, **3**, 1312.
- 5 For leading reviews on "post-metallocene" complexes of groups 3-6 and the lanthanides related to olefin oligo/polymerization, see: (a) G. J. P. Britovsek, V. C. Gibson and D. F. Wass, *Angew. Chem., Int. Ed.*, 1999, **38**, 428; (b) G. W. Coates, P. D. Hustad and S. Reinartz, *Angew. Chem., Int. Ed.*, 2002, **41**, 2236; (c) F. T. Edelman, D. M. M. Freckmann and H. Schumann, *Chem. Rev.*, 2002, **102**, 1851; (d) V. C. Gibson and S. K. Spitzmesser, *Chem. Rev.*, 2003, **103**, 283; (e) J. Gromada, A. Mortreux and J.-F. Carpentier, *Coord. Chem. Rev.*, 2004, **248**, 397; (f) P. Corradini, G. Guerra and L. Cavallo, *Acc. Chem. Res.*, 2004, **37**, 231; (g) M. Kol, S. Segal, S. Groysman in *Stereoselective Polymerization with Single-Site Catalysts*, CRC Press LLC, Boca Raton, Fla, 2008, pp. 345-361; (h) J. Okuda, *Stud. Surf. Sci. Catal.*, 2007, **172**, 11; (i) G. J. Domski, J. M. Rose, G. W. Coates, A. D. Bolig and M. Brookhart, *Prog. Polym. Sci.*, 2007, **32**, 30.
- 6 For leading reviews, see: O. Dechy-Cabaret, B. Martin-Vaca and D. Bourissou, *Chem. Rev.*, 2004, **104**, 6147; (a) B. J. O'Keefe, M. A. Hillmyer and W. B. Tolman, *J. Chem. Soc., Dalton Trans.*, 2001, 2215; (b) J. Wu, T.-L. Yu, C.-T. Chen and C.-C. Lin, *Coord. Chem. Rev.*, 2006, **250**, 602; (c) A. Amgoune, C. M. Thomas and J.-F. Carpentier, *Pure Appl. Chem.*, 2007, **79**, 2013; (d) R. H. Platel, L. M. Hodgson and C. K. Williams, *Polym. Rev.*, 2008, **48**, 11; (e) A. P. Dove, *Chem. Commun.*, 2008, 6446.
- 7 (a) C.-X. Cai, L. Toupet and J.-F. Carpentier, *J. Organomet. Chem.*, 2003, **683**, 131; (b) C.-X. Cai, A. Amgoune, C. W. Lehmann and J.-F. Carpentier, *Chem. Commun.*, 2004, 330; (c) A. Amgoune, C. M. Thomas, T. Roisnel and J.-F. Carpentier, *Chem.-Eur. J.*, 2006, **12**, 169; (d) A. Amgoune, C. M. Thomas, S. Ilinca, T. Roisnel and J.-F. Carpentier, *Angew. Chem., Int. Ed.*, 2006, **45**, 2782; (e) A. Amgoune, C. M. Thomas and J.-F. Carpentier, *Macromol. Rapid Commun.*, 2007, **28**, 693; (f) N. Ajellal, M. Bouyahyi, A. Amgoune, C. M. Thomas, A. Bondon, I. Pillin, Y. Grohens and J.-F. Carpentier, *Macromolecules*, 2009, **42**, 987; (g) H. Ma, T. P. Spaniol and J. Okuda, *Dalton Trans.*, 2003, 4770; (h) H. Y. Ma and J. Okuda, *Macromolecules*, 2005, **38**, 2665; (i) H. Y. Ma, T. P. Spaniol and J. Okuda, *Angew. Chem., Int. Ed.*, 2006, **45**, 7818; (j) H. Ma, T. P. Spaniol and J. Okuda, *Inorg. Chem.*, 2008, **47**, 3328; (k) F. Bonnet, A. R. Cowley and P. Mountford, *Inorg. Chem.*, 2005, **44**, 9046; (l) X. Liu, X. Shang, T. Tang, N. Hu, F. Pei, D. Cui, X. Chen and X. Jing, *Organometallics*, 2007, **26**, 2747; (m) P. I. Binda and E. E. Delbridge, *Dalton Trans.*, 2007, 4685.
- 8 (a) Y. Takashima, Y. Nakayama, K. Watanabe, T. Itono, N. Ueyama, A. Nakamura, H. Yasuda, A. Harada and J. Okuda, *Macromolecules*, 2002, **35**, 7538; (b) Y. Sarazin, R. Howard, D. Hughes, S. Humphrey and M. Bochmann, *Dalton Trans.*, 2006, 340; (c) S. Gendler, S. Segal, I. Goldberg, Z. Goldschmidt and M. Kol, *Inorg. Chem.*, 2006, **45**, 4783; (d) A. J. Chmura, M. G. Davidson, M. D. Jones, M. D. Lunn, M. F. Mahon, A. F. Johnson, P. Khunkamchoo, S. L. Roberts and S. S. F. Wong, *Macromolecules*, 2006, **39**, 7250; (e) A. J. Chmura, M. G. Davidson, C. J. Frankis, M. D. Jones and M. D. Lunn, *Chem. Commun.*, 2008, 1293.
- 9 S. Steinhäuser, U. Heinz, J. Sander and K. Hegetschweiler, *Z. Anorg. Allg. Chem.*, 2004, **630**, 1829.
- 10 Y. Q. Li, Y. Liu, W. M. Bu, J. H. Guo and Y. Wang, *Chem. Commun.*, 2000, 1551.
- 11 (a) E. Kirillov, J.-F. Carpentier and A. Razavi, *Eur. Pat. Appl.*, 2008, 290, p. 410.3; (b) E. Kirillov, T. Roisnel, A. Razavi and J.-F. Carpentier, *Organometallics*, 2009, **28**, 5036.
- 12 The following atom numbering of the naphtholate unit is used:



- 13 For additional examples of ROP of lactide and β -butyrolactone with group 3 metal and lanthanide complexes, see: (a) A. Le Borgne, C. Pluta and N. Spassky, *Macromol. Rapid Commun.*, 1994, **15**, 955; (b) N. Spassky, V. Simic, M. S. Montaudo and L. G. Hubert-Pfalzgraf, *Macromol. Chem. Phys.*, 2000, **201**, 2432; (c) K. B. Aubrecht, K. Chang, M. A. Hillmyer and W. B. Tolman, *J. Polym. Sci., Part A: Polym. Chem.*, 2001, **39**, 284; (d) G. R. Giesbrecht, G. D. Whitener and J. Arnold, *J. Chem. Soc., Dalton Trans.*, 2001, 923; (e) T. M. Oviatt and G. W. Coates, *J. Am. Chem. Soc.*, 2002, **124**, 1316; (f) Y. Satoh, N. Ikitake, Y. Nakayama, S. Okuno and H. Yasuda, *J. Organomet. Chem.*, 2003, **667**, 42; (g) L. Zhang, Z. Shen, C. Yu and L. Fan, *J. Macromol. Sci. Part A: Pure Appl. Chem.*, 2004, **41**, 927; (h) I. Westmoreland and J. Arnold, *Dalton Trans.*, 2006, 4155; (i) A. Alaaeddine, A. Amgoune, C. M. Thomas, S. Dagorne, S. Bellemin-Lapognaz and J.-F. Carpentier, *Eur. J. Inorg. Chem.*, 2006, 3652; (j) J. Wang, T. Cai, Y. Yao and Q. Shen, *Dalton Trans.*, 2007, 5275; (k) S. Wang, S. Wang, S. Zhou, G. Yang, W. Luo, N. Hu, Z. Zhou and H.-B. Song, *J. Organomet. Chem.*, 2007, **692**, 2099; (l) S. Zhou, S. Wang, E. Sheng, L. Zhang, Z. Yu, X. Xi, G. Chen, W. Luo and Y. Li, *Eur. J. Inorg. Chem.*, 2007, 1519; (m) H. Zhou, H. Guo, Y. Yao, L. Zhou, H. Sun, H. Sheng, Y. Zhang and Q. Shen, *Inorg. Chem.*, 2007, **46**, 958; (n) M. T. Gamer, P. W. Roesky, I. Pallard, M. Le Hellaye and S. M. Guillaume, *Organometallics*, 2007, **26**, 651; (o) E. E. Delbridge, D. T. Dugah, C. R. Nelson, B. W. Skelton and A. H. White, *Dalton Trans.*, 2007, 143; (p) G. G. Skvortsov, M. V. Yakovenko, P. M. Castro, G. K. Fukin, A. V. Cherkasov, J.-F. Carpentier and A. A. Trifonov, *Eur. J. Inorg. Chem.*, 2007, 3260; (q) R. Heck, E. Schulz, J. Collin and J.-F. Carpentier, *J. Mol. Catal. A: Chem.*, 2007, **268**, 163; (r) N. Ajellal, D. M. Lyubov, M. A. Sinenkov, G. K. Fukin, A. V. Cherkasov, C. M. Thomas, J.-F. Carpentier and A. A. Trifonov, *Chem.-Eur. J.*, 2008, **14**, 5440; (s) T. V. Mahrova, G. K. Fukin, A. V. Cherkasov, A. A. Trifonov, N. Ajellal and J.-F. Carpentier, *Inorg. Chem.*, 2009, **48**, 4258.
- 14 (a) R. Anwender, O. Runte, J. Eppinger, G. Gerstberger, E. Herdtweck and M. Speigler, *J. Chem. Soc., Dalton Trans.*, 1998, 847; (b) J. Eppinger, M. Speigler, W. Hieringer, W. A. Herrmann and R. Anwender, *J. Am. Chem. Soc.*, 2000, **122**, 3080.
- 15 Note that the C2 and Cs symmetry refers here to the coordination mode of the ligand, but not to the complex because of the position of the amide and THF ligands.
- 16 As revealed by significant broadening of the α -THF hydrogens at intermediate temperatures (*ca.* room temperature), the same dynamic phenomena take place in scandium compound **4**, but the resonances for the diastereotopic α -THF hydrogens appear incidentally isochronic in this case.

- 17 A. Alaaeddine, C. M. Thomas, T. Roisnel and J.-F. Carpentier, *Organometallics*, 2009, **28**, 1469.
- 18 Ionic radii (in Å) for six-coordinated metal centers: Sc^{3+} , 0.75; Y^{3+} , 0.90; La^{3+} , 1.17; Ti^{4+} , 0.61; Zr^{4+} , 0.72; Hf^{4+} , 0.71; Ta^{5+} , 0.64. R. D. Shannon, *Acta Crystallogr., Sect. A: Cryst. Phys., Diff., Theor. Gen. Crystallogr.*, 1976, **A32**, 751.
- 19 T. Agapie, M. W. Day and J. E. Bercaw, *Organometallics*, 2008, **27**, 6123.
- 20 (a) P. N. O'Shaughnessy, P. D. Knight, C. Morton, K. M. Gillespie and P. Scott, *Chem. Commun.*, 2003, 1770; (b) D. V. Gribkov, K. C. Hultsch and F. Hampel, *Chem.-Eur. J.*, 2003, **9**, 4796.
- 21 (a) L. Lavanant, T.-Y. Chou, Y. Chi, C. W. Lehmann, L. Toupet and J.-F. Carpentier, *Organometallics*, 2004, **23**, 5450; (b) E. Grunova, E. Kirillov, T. Roisnel and J.-F. Carpentier, *Organometallics*, 2008, **27**, 5691.
- 22 (a) C. Runschke and G. Meyer, *Z. Anorg. Allg. Chem.*, 1997, **623**, 1493; (b) Y. Li, F.-K. Zheng, X. Liu, W.-Q. Zou, G.-C. Guo, C.-Z. Lu and J.-S. Huang, *Inorg. Chem.*, 2006, **45**, 6308; (c) L. Natrajan, J. Pecaut and M. Mazzanti, *Dalton Trans.*, 2006, 1002.
- 23 In some cases, for convenience, *in situ* combinations of the pro-ligand $\{\text{OZO}^{\text{SiR}_3}\}_2\text{H}_2$ with the tris(amido) precursor were investigated instead of isolated compounds. We independently checked for **2** and **3** that the corresponding *in situ* systems lead to similar polymerization results.
- 24 I. Barakat, P. Dubois, R. Jerome and P. Teyssie, *J. Polym. Sci., Part A: Polym. Chem.*, 1993, **31**, 505–514.
- 25 For low molar mass PLAs generated in the presence of isopropanol, determination of the number-average molar mass by ^1H NMR [from the relative intensity of the signals of the methyl hydrogens of the PLA chains to the methyl hydrogens of the $\text{C}(\text{O})\text{OCH}(\text{CH}_3)_2$ end-groups] gave values in close agreement with those determined by SEC analysis.
- 26 MALDI-ToF-MS analysis of some PLA samples recovered at high monomer conversions (>95%) showed distributions containing both even-membered and odd-membered oligomers, with peaks separated by 72 Da. This unambiguously established that transesterification processes take place in these systems, especially in the later stages of the polymerization.
- 27 (a) For the pioneering work of Inoue in the immortal polymerizations of epoxides initiated with zinc complexes of *N*-substituted porphyrins, see: Y. Watanabe, T. Aida and S. Inoue, *Macromolecules*, 1990, **23**, 2612. For application of this concept to the highly efficient immortal ROP of lactide and cyclic carbonates, see: (b) M. Helou, O. Miserque, J.-M. Brusson, J.-F. Carpentier and S. M. Guillaume, *Chem.-Eur. J.*, 2008, **14**, 8772; (c) V. Poirier, T. Roisnel, J.-F. Carpentier and Y. Sarazin, *Dalton Trans.*, 2009, 9820.
- 28 Detailed microstructural analysis of the PLAs by ^{13}C NMR spectroscopy, comparing the experimental triad/tetrad resonance intensities with those calculated from a Bernoullian statistics, gave results consistent with a chain-end stereocontrol mechanism. For instance, Table 3, entry 5 (resonance, experimental/calculated): *rmr*, 0.35/0.39; *rmm/nmr*, 0.07/0.05; *nmr/rmm*, 0.08/0.05; *mrm+mmm*, 0.50/0.44+0.07. See: (a) K. A. M. Thakur, R. T. Kean, E. S. Hall, J. J. Kolstad, T. A. Lindgren, M. A. Doscotch, J. I. Siepmann and E. J. Munson, *Macromolecules*, 1997, **30**, 2422; (b) K. A. M. Thakur, R. T. Kean, E. S. Hall, J. J. Kolstad, T. A. Lindgren, M. A. Doscotch, J. I. Siepmann and E. J. Munson, *Macromolecules*, 1998, **31**, 1487; (c) K. A. M. Thakur, R. T. Kean, M. T. Zell, B. E. Padden and E. J. Munson, *Chem. Commun.*, 1998, 1913; (d) M. H. Chisholm, S. S. Iyer, D. G. McCollum, M. Pagel and U. Werner-Zwanziger, *Macromolecules*, 1999, **32**, 963.
- 29 The comparison of theoretical with experimental M_n values must be done with caution since the latter values are uncorrected and might be overestimated. However, no reliable correction factor accounting for the difference in hydrodynamic radius between PHBs and polystyrene standards has been reported to our knowledge. SEC analysis of higher molecular weight PHBs is known to be problematic. See reference 7f and references cited therein.
- 30 A. Altomare, M. C. Burla, M. Camalli, G. Casciarano, C. Giacovazzo, A. Guagliardi, A. G. G. Moliterni, G. Polidori and R. Spagna, *J. Appl. Crystallogr.*, 1999, **32**, 115.
- 31 (a) G. M. Sheldrick *SHELXS-97, Program for the Determination of Crystal Structures*, University of Goettingen (Germany), 1997; (b) G. M. Sheldrick *SHELXL-97, Program for the Refinement of Crystal Structures*, University of Goettingen (Germany), 1997.
- 32 L. J. Farrugia, *J. Appl. Crystallogr.*, 1999, **32**, 837.
- 33 P. Van Der Sluis and A. L. Spek, *Acta Crystallogr., Sect. A: Found. Crystallogr.*, 1990, **A46**, 194.
- 34 A. L. Spek, *Acta Crystallogr.*, 1990, **A46**, C-34.